

Preheating after Multifield Inflation with Nonminimal Couplings, I: Covariant Formalism and Attractor Behavior

Matthew P. DeCross¹, David I. Kaiser¹, Anirudh Prabhu¹,

C. Prescod-Weinstein¹, and Evangelos I. Sfakianakis^{2*}

¹*Department of Physics, Massachusetts Institute of Technology, Cambridge, Massachusetts 02139 USA*

²*Department of Physics, University of Illinois at Urbana-Champaign, Urbana, Illinois 61801*

(Dated: November 29, 2015)

We study the preheating phase for multifield models of inflation involving nonminimal couplings. The strong single-field attractor behavior during inflation in these models generically persists after the end of inflation, thereby avoiding the “de-phasing” that is typical in multifield models with minimally coupled scalar fields. Hence we find efficient transfer of energy from the oscillating inflaton field(s) to coupled fluctuations. We develop a doubly-covariant formalism for studying such resonances and identify several features of preheating specific to the nonminimal couplings, including effects that arise from the nontrivial field-space manifold. In particular, whereas long-wavelength fluctuations in both the adiabatic and isocurvature directions may be resonantly amplified for small or modest values of the dimensionless nonminimal couplings, $\xi_I \leq 1$, we find suppression of the growth of long-wavelength isocurvature modes in the limit of strong coupling, $\xi_I \gg 1$.

PACS numbers: 98.80.Cq ; 95.30.Cq. Preprint MIT-CTP/4716.

I. INTRODUCTION

Post-inflation reheating is a critical phase in the history of the cosmos, necessary to connect early-universe inflation to the usual successes of the standard hot big bang scenario. Reheating falls between two regimes that are well constrained by observations, and which match the latest observations remarkably well: production of a spatially flat universe seeded with nearly scale-invariant primordial curvature perturbations during inflation [1–8], and production of specific abundances of light nuclei during big-bang nucleosynthesis [9–11]. Though it remains difficult to relate the reheating phase directly to specific, testable predictions for observations, the process of reheating remains critical in order to compare predictions from the inflationary era with present-day observations, since relating comoving scales at different cosmological epochs requires knowledge of the

* Email addresses: mdecross@mit.edu ; dikaiser@mit.edu ; aprabhu@mit.edu ; chanda@mit.edu ; esfaki@illinois.edu

intervening expansion history of the universe [12–18]. See [2, 19–21] for recent reviews of reheating.

The post-inflation reheating phase not only must bring the early universe to thermal equilibrium in a radiation-dominated phase at an appropriately high temperature; reheating should also populate the universe with matter like the kind we see around us today. During inflation, the energy density of the universe was presumably dominated by one or more scalar “inflaton” fields. After reheating, the energy density should include contributions from multiple species of matter, including the Standard Model particles or (at least) types of matter that decay into Standard Model particles prior to big-bang nucleosynthesis; such interactions could address other long-standing challenges in cosmological theory, such as generating the observed baryon - antibaryon asymmetry [22–24]. Reheating therefore must be a multifield phenomenon.

Arguably, inflation itself should be treated as a process involving multiple fields. Realistic models of high-energy particle physics typically include many distinct scalar fields at high energies [25–27]. Hence we consider multiple scalar fields to be a central ingredient of realistic models of inflation. Nonminimal couplings between the scalar fields and the Ricci spacetime curvature scalar are also a generic feature of realistic models of the early universe. Many theoretical motivations for nonminimal couplings derive from high-energy model-building, including dilatons and moduli fields, but a more basic motivation comes from renormalization: as has long been known, models with self-interacting scalar fields in curved spacetime require nonminimal couplings as counterterms in order to remain self-consistent at high energies. Nonminimal couplings are induced by quantum corrections even in the absence of bare couplings; they are a generic feature of scalar fields in curved spacetime [28–32].

In recent work [33–36] we have studied the dynamics during inflation from multifield models with nonminimal couplings, including generalizations of “Higgs inflation” [37]. These papers have demonstrated that such models generically predict observable quantities (related to the spectrum of primordial curvature perturbations) squarely in the most-favored region of the latest observations. In fact, such models exhibit a strong attractor behavior: across broad regions of parameter space and phase space the fields relax to an effectively single-field trajectory early in inflation. Hence the predictions for observable quantities from these models show little dependence on coupling constants or initial conditions [35]. Such attractor behavior is a generic feature of multifield models with nonminimal couplings, including the recently identified family of “ α attractors” [38].

In this paper we focus on the dynamics of such models immediately after inflation, during the “preheating” phase. During preheating, the scalar-field condensate(s) that drove inflation decay resonantly into higher-momentum quanta. We develop a doubly-covariant formalism that incorpo-

rates metric perturbations and field fluctuations self-consistently (to first order), and which also respects the reparameterization freedom of the nontrivial field-space manifold. We restrict attention to the early stages of preheating, for which an approximation linear in the fields' fluctuations remains reliable, and only consider decays into scalar fields rather than fermions or gauge fields. Our approach complements previous studies that have examined reheating in models with nonminimally coupled fields [39–42], including Higgs inflation [43–46], as well as with noncanonical kinetic terms [47–50]. In a companion paper [51], we analyze the structure of resonances in this family of models semi-analytically and numerically across wide regions of parameter space.

We find three principal distinctions from the well-studied cases of preheating with minimally coupled fields. First, the conformal stretching of the scalar fields' potential in the Einstein frame affects the oscillations of the background fields, compared to the case of minimal couplings. In particular, for strong nonminimal couplings $\xi_I \gg 1$, the background fields' oscillations interpolate between the behavior of minimally coupled models with quadratic and quartic self-couplings. Second, the single-field attractor behavior during inflation leads to greater efficiency during preheating than in corresponding multifield models with minimal couplings, in which de-phasing of the background fields' oscillations typically damps resonances [21, 52, 53]. Third, in the limit of strong couplings, $\xi_I \gg 1$, the nontrivial field-space manifold contributes differently to the effective masses for fluctuations in the adiabatic and isocurvature directions, limiting the transfer of energy to long-wavelength isocurvature perturbations.

In Section II we briefly review the doubly-covariant formalism with which we study the dynamics of background fields and fluctuations. In Section III we examine the background dynamics for a two-field model during and after inflation, highlighting distinctions between oscillations during preheating with and without nonminimal couplings. The behavior of the background fields during the oscillating phase is critical for understanding the resonant production of particles during preheating. In Section IV we introduce a covariant mode expansion for the fluctuations and derive multifield generalizations of the “adiabatic parameter” with which to characterize the resonant, nonperturbative growth of fluctuations. Concluding remarks follow in Section V.

II. DOUBLY-COVARIANT FORMALISM

When studying multifield models with nonminimal couplings, one must consider two types of gauge transformations: the usual spacetime coordinate transformations, $x^\mu \rightarrow x^{\mu'}$, as well as transformations of the field-space coordinates, $\phi^I \rightarrow \phi^{I'}$. To address the first type of transformation,

we adopt the usual (spacetime) gauge-invariant perturbation formalism [56–58]; see [2, 59, 60] for reviews. To address the multifield aspects, we build on the methods of [61–72]. Together, these yield a doubly-covariant formalism for studying fluctuations in these multifield models [33].

We follow closely the notation and parameterization of [33–36]. We work in $(3+1)$ spacetime dimensions and adopt the spacetime metric signature $(-, +, +, +)$. We consider models with N real-valued scalar fields, each of which is coupled to the Ricci spacetime curvature scalar. In the Jordan frame, the action takes the form

$$S = \int d^4x \sqrt{-\tilde{g}} \left[f(\phi^I) \tilde{R} - \frac{1}{2} \delta_{IJ} \tilde{g}^{\mu\nu} \partial_\mu \phi^I \partial_\nu \phi^J - \tilde{V}(\phi^I) \right], \quad (1)$$

where upper-case Latin letters label field-space indices, $I, J = 1, 2, \dots, N$, Greek letters label space-time indices, $\mu, \nu = 0, 1, 2, 3$, and tildes denote Jordan-frame quantities. We will use lower-case Latin letters for spatial indices, $i, j = 1, 2, 3$.

We may perform a conformal transformation to bring the gravitational portion of the action into canonical Einstein-Hilbert form, by rescaling $\tilde{g}_{\mu\nu}(x) \rightarrow g_{\mu\nu}(x) = \Omega^2(x) \tilde{g}_{\mu\nu}(x)$. The conformal factor $\Omega^2(x)$ is related to the nonminimal-coupling function,

$$g_{\mu\nu}(x) = \frac{2}{M_{\text{pl}}^2} f(\phi^I(x)) \tilde{g}_{\mu\nu}(x), \quad (2)$$

where $M_{\text{pl}} \equiv 1/\sqrt{8\pi G} = 2.43 \times 10^{18}$ GeV is the reduced Planck mass. The action may then be rewritten [55]

$$S = \int d^4x \sqrt{-g} \left[\frac{M_{\text{pl}}^2}{2} R - \frac{1}{2} \mathcal{G}_{IJ}(\phi^K) g^{\mu\nu} \partial_\mu \phi^I \partial_\nu \phi^J - V(\phi^I) \right]. \quad (3)$$

The potential in the Einstein frame is stretched by the conformal factor,

$$V(\phi^I) = \frac{M_{\text{pl}}^4}{4f^2(\phi^I)} \tilde{V}(\phi^I). \quad (4)$$

In addition, the nonminimal couplings induce a curved field-space manifold in the Einstein frame, with associated field-space metric $\mathcal{G}_{IJ}(\phi^K)$. Because the induced field-space manifold is not conformal to flat $N \geq 2$, no combination of rescalings of $g_{\mu\nu}$ and ϕ^I can retain the Einstein-Hilbert form for the gravitational portion of the action while also bringing the fields' kinetic terms into canonical form [55]. The components of \mathcal{G}_{IJ} take the form

$$\mathcal{G}_{IJ}(\phi^K) = \frac{M_{\text{pl}}^2}{2f(\phi^K)} \left[\delta_{IJ} + \frac{3}{f(\phi^K)} f_{,I} f_{,J} \right], \quad (5)$$

where $f_{,I} = \partial f / \partial \phi^I$. The field-space metric satisfies $\mathcal{G}^{IJ} \mathcal{G}_{JK} = \delta_K^I$, and field-space indices are raised and lowered with \mathcal{G}_{IJ} .

Varying the action of Eq. (3) with respect to $g_{\mu\nu}$ yields the field equations

$$R_{\mu\nu} - \frac{1}{2}g_{\mu\nu}R = \frac{1}{M_{\text{pl}}^2}T_{\mu\nu}, \quad (6)$$

with the energy-momentum tensor given by [33]

$$T_{\mu\nu} = \mathcal{G}_{IJ}\partial_\mu\phi^I\partial_\nu\phi^J - g_{\mu\nu}\left[\frac{1}{2}\mathcal{G}_{IJ}g^{\alpha\beta}\partial_\alpha\phi^I\partial_\beta\phi^J + V(\phi^I)\right]. \quad (7)$$

Varying Eq. (3) with respect to ϕ^I yields the equation of motion

$$\square\phi^I + g^{\mu\nu}\Gamma_{JK}^I\partial_\mu\phi^J\partial_\nu\phi^K - \mathcal{G}^{IJ}V_{,J} = 0, \quad (8)$$

where $\square\phi^I \equiv g^{\mu\nu}\phi^I_{;\mu\nu}$ and $\Gamma_{JK}^I(\phi^L)$ is the Christoffel symbol constructed from the field-space metric \mathcal{G}_{IJ} .

We expand the scalar fields and the spacetime metric to first order in perturbations. We are interested in the behavior of the fields at the end of inflation, so we consider scalar metric perturbations around a spatially flat Friedmann-Lemaître-Robertson-Walker (FLRW) line element,

$$\begin{aligned} ds^2 &= g_{\mu\nu}(x) dx^\mu dx^\nu \\ &= -(1 + 2A)dt^2 + 2a(\partial_i B) dx^i dt + a^2[(1 - 2\psi)\delta_{ij} + 2\partial_i\partial_j E] dx^i dx^j, \end{aligned} \quad (9)$$

where $a(t)$ is the scale factor. We also expand the fields,

$$\phi^I(x^\mu) = \varphi^I(t) + \delta\phi^I(x^\mu). \quad (10)$$

The fluctuations $\delta\phi^I$ represent finite displacements from the fields' classical trajectory through field space; the fluctuations $\delta\phi^I$ are gauge dependent with respect to both $x^\mu \rightarrow x^{\mu'}$ and $\varphi^I \rightarrow \varphi^{I'}$. We therefore proceed in two steps. First, following [71], we introduce a vector \mathcal{Q}^I to represent the field fluctuations covariantly with respect to the field-space metric, \mathcal{G}_{IJ} . (See also [72].) The field-space vectors $\phi^I(x^\mu)$ and $\varphi^I(t)$ may be connected by a geodesic along the field-space manifold with some affine parameter λ . We take $\phi^I(\lambda = 0) = \varphi^I$ and $\phi^I(\lambda = \epsilon) = \varphi^I + \delta\phi^I$. (We may take $\epsilon = 1$ at the end.) These boundary conditions uniquely specify the vector \mathcal{Q}^I that connects ϕ^I and φ^I , such that $\phi^I|_{\lambda=0} = \varphi^I$ and $\mathcal{D}_\lambda\phi^I|_{\lambda=0} = (d\phi^I/d\lambda)|_{\lambda=0} = \mathcal{Q}^I$, where \mathcal{D}_λ is a covariant derivative with respect to the affine parameter. Then [71]

$$\delta\phi^I = \mathcal{Q}^I - \frac{1}{2!}\Gamma_{JK}^I\mathcal{Q}^J\mathcal{Q}^K + \frac{1}{3!}[\Gamma_{LM}^I\Gamma_{JK}^M - \Gamma_{JK;L}^I]\mathcal{Q}^J\mathcal{Q}^K\mathcal{Q}^L + \dots \quad (11)$$

where the Γ_{JK}^I are evaluated at background order, as functions of φ^I . Note that $\delta\phi^I \rightarrow \mathcal{Q}^I$ to first order in fluctuations, but one must take care to distinguish the two when working to higher order,

as we will do in Section IV A when we expand the action to second order in Q^I . Next, we follow [33] and define a linear combination of Q^I and the metric perturbation ψ to form a generalization of the gauge-invariant Mukhanov-Sasaki variable:

$$Q^I \equiv \mathcal{Q}^I + \frac{\dot{\phi}^I}{H} \psi. \quad (12)$$

The vector Q^I is doubly covariant, with respect to spacetime gauge transformations (to first order in metric perturbations) as well as transformations of the field-space coordinates φ^I . To first order in perturbations, $Q^I \rightarrow \mathcal{Q}^I \rightarrow \delta\phi^I$ in the spatially flat gauge.

For an arbitrary vector in the field space, A^I , we may define the usual covariant derivative with respect to the field-space metric,

$$\mathcal{D}_J A^I = \partial_J A^I + \Gamma_{JK}^I A^K, \quad (13)$$

and a (covariant) directional derivative with respect to the affine parameter, cosmic time, t ,

$$\mathcal{D}_t A^I \equiv \dot{\phi}^J \mathcal{D}_J A^I = \dot{A}^I + \Gamma_{JK}^I \dot{\phi}^J A^K, \quad (14)$$

where overdots denote partial derivatives with respect to t . To background order, we may then write the equation of motion for the fields φ^I from Eq. (8),

$$\mathcal{D}_t \dot{\phi}^I + 3H \dot{\phi}^I + \mathcal{G}^{IJ} V_{,J} = 0, \quad (15)$$

while Eqs. (6)-(7) yield the usual dynamical equations at background order,

$$\begin{aligned} H^2 &= \frac{1}{3M_{\text{pl}}^2} \left[\frac{1}{2} \mathcal{G}_{IJ} \dot{\phi}^I \dot{\phi}^J + V(\varphi^I) \right], \\ \dot{H} &= -\frac{1}{2M_{\text{pl}}^2} \mathcal{G}_{IJ} \dot{\phi}^I \dot{\phi}^J. \end{aligned} \quad (16)$$

In Eqs. (15)-(16), $H \equiv \dot{a}/a$ is the Hubble parameter, and the field-space metric is evaluated at background order, $\mathcal{G}_{IJ}(\varphi^K)$.

To first order in Q^I , Eqs. (6)-(8) may be combined to yield the equation of motion for the gauge-invariant perturbations [33, 54, 69]

$$\mathcal{D}_t^2 Q^I + 3H \mathcal{D}_t Q^I + \left[\frac{k^2}{a^2} \delta_{IJ}^I + \mathcal{M}_{IJ}^I \right] Q^J = 0, \quad (17)$$

where the mass-squared tensor takes the form

$$\mathcal{M}_{IJ}^I \equiv \mathcal{G}^{IK} (\mathcal{D}_J \mathcal{D}_K V) - \mathcal{R}_{LMJ}^I \dot{\phi}^L \dot{\phi}^M - \frac{1}{M_{\text{pl}}^2 a^3} \mathcal{D}_t \left(\frac{a^3}{H} \dot{\phi}^I \dot{\phi}^J \right) \quad (18)$$

and \mathcal{R}_{LMJ}^I is the Riemann tensor for the field-space manifold. All expressions in Eqs. (17) and (18) involving \mathcal{G}_{IJ} , V , and their derivatives are evaluated at background order in the fields, φ^I . The term in Eq. (18) that is proportional to $1/M_{\text{pl}}^2$ arises from the coupled metric perturbations.

III. COUPLINGS AND BACKGROUND DYNAMICS

Renormalization of models with self-coupled scalar fields in curved spacetime requires counter-terms of the form $\xi\phi^2 R$ for each nonminimally coupled field [28–32]. Here we consider a two-field model, $\phi^I = (\phi, \chi)^T$, and take $f(\phi^I)$ to be of the form

$$f(\phi, \chi) = \frac{1}{2} [M_{\text{pl}}^2 + \xi_\phi \phi^2 + \xi_\chi \chi^2]. \quad (19)$$

Each scalar field ϕ^I couples to the Ricci scalar with its own nonminimal-coupling constant, ξ_I ; conformal coupling corresponds to $\xi_I = -1/6$. The field-space metric, $\mathcal{G}_{IJ}(\varphi^K)$, is determined by the form of $f(\phi^I)$ and its derivatives, as in Eq. (5). Explicit expressions for \mathcal{G}_{IJ} and related quantities for this model may be found in Appendix A.

We consider a simple, renormalizable form for the potential in the Jordan frame,

$$\tilde{V}(\phi, \chi) = \frac{\lambda_\phi}{4} \phi^4 + \frac{g}{2} \phi^2 \chi^2 + \frac{\lambda_\chi}{4} \chi^4. \quad (20)$$

We take $\lambda_I > 0$ and neglect bare masses m_I^2 , in order to focus on effects from the quartic self-couplings and direct interaction terms within a parameter space of manageable size. The effects from nonzero m_I^2 may be incorporated in later studies using the methods developed here.

Several types of considerations may be used to bound the range of ξ_I of interest. Perhaps most fundamentally, vacuum stability (under renormalization-group flow) requires $\xi_I \geq -0.03$ [76]. Meanwhile, earlier studies of single-field models had found that $|\xi| \leq 10^{-3}$ for $\xi < 0$ in order to yield sufficient inflation [77–81]. Hence we restrict attention here to positive couplings, $\xi_I > 0$.

Next we may consider observational constraints, such as the present bound on the primordial tensor-to-scalar ratio, $r \leq 0.1$ [82], which corresponds to the bound $H_* \leq 3.4 \times 10^{-5} M_{\text{pl}}$. (Asterisks indicate values of quantities at the time during inflation when observationally relevant perturbations first crossed outside the Hubble radius.) Models in our class predict [33–36]

$$r = \frac{16\epsilon}{1 + T_{\mathcal{RS}}^2}, \quad (21)$$

where ϵ is the usual slow-roll parameter,

$$\epsilon \equiv -\frac{\dot{H}}{H^2}, \quad (22)$$

and $T_{\mathcal{RS}}^2$ is the transfer function for long-wavelength modes between the adiabatic (\mathcal{R}) and isocurvature (\mathcal{S}) directions. As analyzed in [33–36] and discussed further in the next section, models in this class generically display strong single-field attractor behavior. Within an attractor the background fields’ trajectory does not turn, and hence $T_{\mathcal{RS}}^2 \rightarrow 0$. Furthermore, given our covariant

framework, we may consider the case in which the fields move along the direction $\chi = 0$ during inflation without loss of generality. In the limit $\xi_\phi \gg 1$, we find to good approximation [35]

$$H_* \simeq \sqrt{\frac{\lambda_\phi}{12\xi_\phi^2}} M_{\text{pl}}, \quad N_* \simeq \frac{3}{4}\delta_*^2, \quad \epsilon \simeq \frac{3}{4N_*^2}, \quad (23)$$

where

$$\delta^2 \equiv \frac{\xi_\phi \phi^2}{M_{\text{pl}}^2}, \quad (24)$$

and N_* is the number of efolds before the end of inflation when relevant scales crossed outside the Hubble radius. Assuming $50 \leq N_* \leq 60$, we find $r \sim \mathcal{O}(10^{-3})$ in the limit $\xi_\phi \gg 1$, and $H_* \leq 3.4 \times 10^{-5} M_{\text{pl}}$ for $\lambda_\phi/\xi_\phi^2 \leq 1.4 \times 10^{-8}$. In models like Higgs inflation [37], one typically finds $\lambda_\phi \sim \mathcal{O}(10^{-2} - 10^{-4})$ at the energy scales of inflation (the range stemming from uncertainty in the value of the top-quark mass, which affects the running of λ_ϕ under renormalization-group flow) [73–75]. The range of λ_ϕ , in turn, requires $\xi_\phi \sim \mathcal{O}(10^2 - 10^3)$ at high energies — a reasonable range, given that ξ_ϕ typically rises with energy scale under renormalization-group flow with no UV fixed point [31]. Even for such large values of ξ_I , the inflationary dynamics occur at energy scales well below any nontrivial unitarity cut-off scale. (See [36] and references therein for further discussion.)

For the opposite limit, with $0 < \xi_\phi \ll 1$, a similar analysis yields [81]

$$H_* \simeq \sqrt{\frac{\lambda_\phi}{12\xi_\phi^2}} \frac{\delta_*^4}{(1 + \delta_*^2)^2} M_{\text{pl}}, \quad N_* \simeq \frac{1}{8\xi_\phi} \delta_*^2, \quad \epsilon \simeq \frac{1}{N_*(1 + 8\xi_\phi N_*)}, \quad (25)$$

where δ^2 is again defined as in Eq. (24). In this limit, the bound $r \leq 0.1$ requires $\xi_\phi \geq 0.006$ (for $N_* = 50$) or $\xi_\phi \geq 0.004$ (for $N_* = 60$), which in turn yields a constraint on λ_ϕ typical of minimally coupled models: $\lambda_\phi \sim \mathcal{O}(10^{-12})$ in order to keep $H_* \leq 3.4 \times 10^{-5} M_{\text{pl}}$ [83, 84]. Thus in the remainder of this analysis, we restrict attention to the range $10^{-3} \leq \xi_I \leq 10^3$.

A. Single-Field Attractor

Inflation begins in a regime in which $\xi_J(\phi^J)^2 > M_{\text{pl}}^2$ for at least one component, J . The potential in the Einstein frame becomes asymptotically flat along each direction of field space, as each field ϕ^I becomes arbitrarily large:

$$V(\phi^I) \rightarrow \frac{M_{\text{pl}}^4}{4} \frac{\lambda_I}{\xi_I^2} \left[1 + \mathcal{O}\left(\frac{M_{\text{pl}}^2}{\xi_I(\phi^I)^2}\right) \right] \quad (26)$$

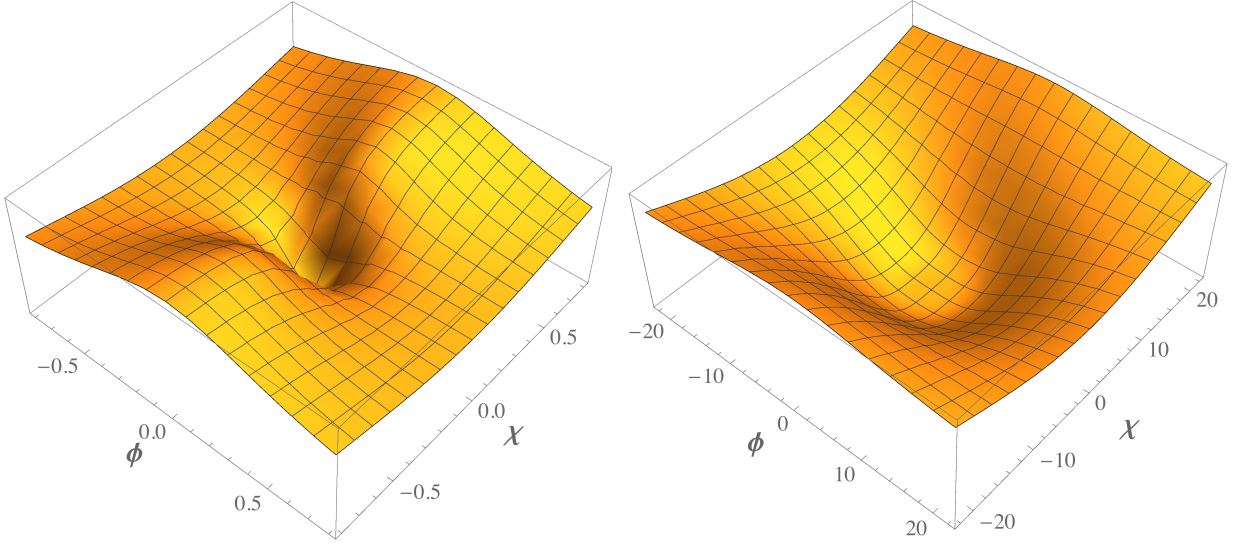


FIG. 1: Potential in the Einstein frame, $V(\phi^I)$, for a two-field model with $\xi_\chi/\xi_\phi = 0.8$, $\lambda_\chi/\lambda_\phi = 1.25$, $g/\lambda_\phi = 1$, and $\xi_\chi = 0.8 \xi_\phi$ for $\xi_\phi = 10^2$ (left) and $\xi_\phi = 10^{-2}$ (right). Field values are in units of M_{pl} .

(no sum on I). Unless some explicit symmetry constrains all coupling constants in the model to be identical ($\lambda_I = g = \lambda$, $\xi_I = \xi$), then the potential in the Einstein frame will develop ridges and valleys. Both the ridges and the valleys satisfy $V > 0$, and hence the system will inflate (albeit at different rates) whether the fields evolve along a ridge or a valley toward the global minimum of the potential. As seen in Fig. 1, even in the case of $\xi_I \ll 1$, in which inflation can occur for field values ϕ^I for which the potential has not reached its asymptotically flat form, the potential still exhibits ridges and valleys, all of which are capable of supporting inflation.

Given the distinct ridge-valley structure of the effective potential in the Einstein frame, these models display strong single-field attractor behavior during inflation, across a wide range of couplings and initial conditions [35]. If the fields happen to begin evolving along the top of a ridge, they will eventually fall into a neighboring valley at a rate that depends on the local curvature of the potential [33, 36]. Once the fields fall into a valley, Hubble drag quickly damps out any transverse motions in field space within a few efolds, after which the system evolves with virtually no turning in field space for the remainder of inflation [33–36]. As shown in Fig. 2, the single-field attractor behavior is as generic in the limit $\xi_I < 1$ as it is for $\xi_I \gg 1$. For all of the trajectories shown, the fields settle into a single-field attractor prior to the last 65 efolds of inflation.

Within a single-field attractor, these models predict values for spectral observables such as the primordial spectral index and its running (n_s and α), the ratio of power in tensor to scalar modes (r), primordial non-Gaussianity (f_{NL}), and the fraction of power in isocurvature rather than

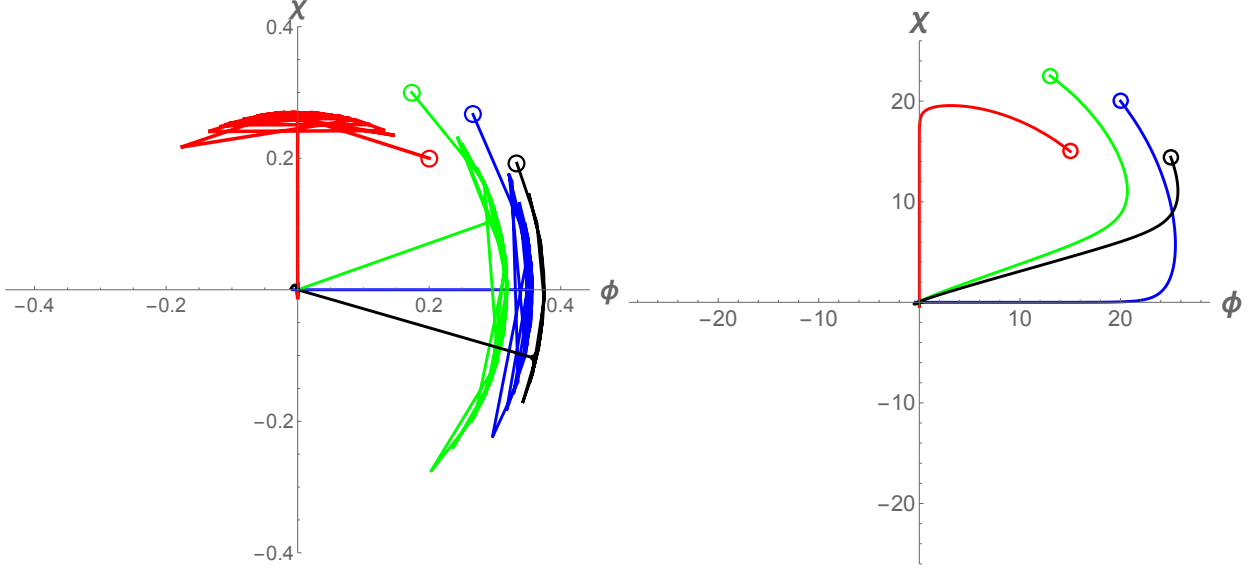


FIG. 2: Field trajectories for different couplings and initial conditions. Open circles indicate fields' initial values (in units of M_{pl}). We set the fields' initial velocities to zero and vary the initial angle in field space, $\theta_0 \equiv \arctan(\chi_0/\phi_0)$. For the figure on the left, we set $\xi_\phi = 10^3$ and $\lambda_\phi = 10^{-2}$; for the figure on the right, we set $\xi_\phi = 10^{-1}$ and $\lambda_\phi = 10^{-10}$. In both figures, the other parameters $\{\xi_\chi, \lambda_\chi, g, \theta_0\}$ are: $\{1.2\xi_\phi, 0.75\lambda_\phi, \lambda_\phi, \pi/4\}$ (red); $\{0.8\xi_\phi, \lambda_\phi, \lambda_\phi, \pi/4\}$ (blue); $\{0.8\xi_\phi, \lambda_\phi, 0.75\lambda_\phi, \pi/3\}$ (green); $\{0.8\xi_\phi, 1.2\lambda_\phi, 0.75\lambda_\phi, \pi/6\}$ (black). In each case, the initial transient motion damps out within a few efolds, yielding effectively single-field evolution for (at least) the final 65 efolds of inflation.

adiabatic scalar modes (β_{iso}) all in excellent agreement with the latest observations [33–36]. Fig. 3 shows the tensor-to-scalar ratio r and the isocurvature fraction β_{iso} as a function of the nonminimal coupling. The approach to a constant ξ_I -independent value for large ξ_I is evident. The fields will only fail to settle into a single-field attractor during inflation if *both* the ratios of certain coupling constants *and* the fields' initial conditions are fine-tuned. If the fields happen to begin very close to the top of a ridge, for example, and if the local curvature of the potential in the vicinity of that ridge has been fine-tuned to be small ($\mathcal{D}_{IJ}V/H^2 \ll 1$), then the system can exhibit significant turning in field space late in inflation [33, 35, 36]. In such fine-tuned cases, the system's evolution during the last 65 efolds of inflation can amplify non-Gaussianities and isocurvature perturbations, which could potentially be observable [33, 36, 54].

In [36] we analyzed the geometric structure of the attractor in the limit $\xi_I \gg 1$; here we generalize that analysis for arbitrary positive ξ_I . As in [36], we define convenient combinations of couplings,

$$\Lambda_\phi \equiv \lambda_\phi \xi_\chi - g \xi_\phi, \quad \Lambda_\chi \equiv \lambda_\chi \xi_\phi - g \xi_\chi, \quad \varepsilon \equiv \frac{\xi_\phi - \xi_\chi}{\xi_\phi}, \quad (27)$$

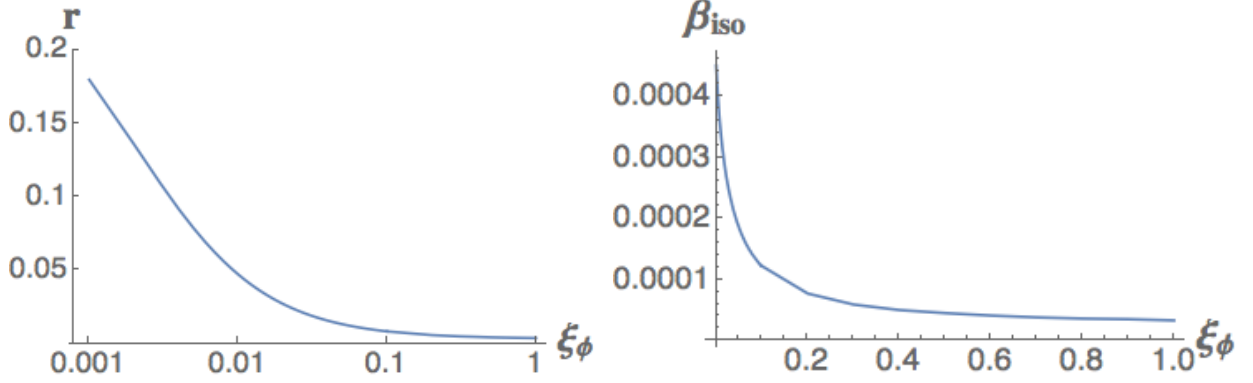


FIG. 3: The tensor-to-scalar ratio (*left*) and the fraction of isocurvature modes (*right*) as a function of the nonminimal coupling ξ_ϕ . The isocurvature fraction is calculated for the symmetric (Higgs-like) case $\lambda_\phi = g = \lambda_\chi$ and $\xi_\phi = \xi_\chi$.

along with the new rescaled quantities

$$\tilde{\Lambda}_\phi \equiv \frac{\Lambda_\phi}{\lambda_\phi \xi_\phi} = \frac{\xi_\chi}{\xi_\phi} - \frac{g}{\lambda_\phi}, \quad \tilde{\Lambda}_\chi \equiv \frac{\Lambda_\chi}{\lambda_\chi \xi_\chi} = \frac{\xi_\phi}{\xi_\chi} - \frac{g}{\lambda_\chi}. \quad (28)$$

For arbitrary $\xi_I > 0$, we find

$$\mathcal{D}_{\chi\chi}V|_{\chi=0} = \frac{\lambda_\phi \phi^2}{[1 + \delta^2]^3 [1 + (1 + 6\xi_\phi)\delta^2]} \left[-\tilde{\Lambda}_\phi (1 + 6\xi_\phi) (\delta^2 + \delta^4) - (\tilde{\Lambda}_\phi + \varepsilon) \delta^2 + \frac{g}{\lambda_\phi} \right], \quad (29)$$

where $\delta^2 \equiv \xi_\phi \phi^2 / M_{\text{pl}}^2$ as in Eq. (24). In the limit $\xi_I \gg 1$, the quantity $\delta^2 \gg 1$ during inflation, and we find $\mathcal{D}_{\chi\chi}V|_{\chi=0} \propto -\Lambda_\phi$, as in [36]. In that limit, whenever $\Lambda_\phi < 0$ the direction $\chi = 0$ remains a local minimum of the potential and the background dynamics will obey strong attractor behavior along the direction $\chi = 0$. For $\xi_I \ll 1$, on the other hand, $\delta^2 \gtrsim 2$ during inflation, as may be seen from the scaling relationships in Eq. (25), and the orientation $\theta = \arctan(\chi/\phi)$ of the local minimum depends on the ellipticity, ε , and the ratio g/λ_ϕ in addition to the sign of Λ_ϕ . Even in these cases, the existence of attractor solutions remains generic (as shown in Fig. 2), only the orientation of the attractor in field space changes. For $\xi_I \ll 1$ there are special regions of parameter space for the coupling values where the topography of the potential can change during inflation, meaning that a ridge can turn into a valley as the inflaton rolls. Depending on the curvature, a waterfall-type transition may occur [85]. We defer this discussion for [51], and restrict the present analysis to the case in which the ridge-valley topography remains consistent throughout inflation.

The orientation of the valley of the potential in field space, $\theta = \arctan(\chi/\phi)$, depends on combinations of couplings λ_I, g , and ξ_I [36, 51]. When studying inflationary dynamics in multifield models, one typically projects physical quantities into adiabatic and isocurvature directions based on the motion of the background fields, φ^I [2, 62–65, 67, 70]. For our two-field model, we may

define the orthogonal unit vectors [33–36]

$$\hat{\sigma}^I \equiv \frac{\dot{\varphi}^I}{\dot{\sigma}}, \quad \hat{s}^I \equiv \frac{\omega^I}{\omega} \quad (30)$$

in terms of the magnitude of the background fields' velocity, $\dot{\sigma}$, and their (covariant) turn-rate,

$$\dot{\sigma} \equiv |\dot{\varphi}^I| = \sqrt{\mathcal{G}_{IJ}\dot{\varphi}^I\dot{\varphi}^J}, \quad \omega^I \equiv \mathcal{D}_t \hat{\sigma}^I. \quad (31)$$

We may then project any field-space vector into adiabatic (σ) and isocurvature (s) components,

$$A_\sigma \equiv \hat{\sigma}_I A^I, \quad A_s \equiv \hat{s}_I A^I. \quad (32)$$

Within a single-field attractor, $\omega^I \rightarrow 0$, so that a vector in field space that lies along the adiabatic direction at one time will continue to point along the adiabatic direction at later times. In that case, we may exploit the covariant nature of our framework to perform a rotation in field space, $\varphi^I \rightarrow \varphi'^I$, such that the valley of the potential lies along the direction $\chi' = 0$. Then the attractor will keep $\chi' \sim \dot{\chi}' \sim 0$, and only $\phi'(t)$ will evolve. With respect to the new field-space coordinates $\{\phi', \chi'\}$, the adiabatic direction points along ϕ' and the isocurvature direction along χ' .

We now review the tools needed to quantify the strength of the attractor by examining the amount of fine-tuning needed to evade it. We will concentrate on the large- ξ_I regime, as it is enough to show the trend in the attractor's strength as a function of ξ_I . Following the analysis of [36] for the case where the fields φ^I start exponentially close to the top of a ridge, we will use the linearized equations of motion to study the strength of the attractor. Apart from the fine-tuned curvature of the ridge ($\tilde{\Lambda}_\phi$), the dynamics of the inflaton field, which is translated into the attractor strength, depend very sensitively on the initial proximity to the top of the ridge. The obvious universal parameter of the proximity to the top of the ridge is the angle in field space, θ . The initial angle is $\theta_0 \approx \chi_0/\phi_0$ for $\chi_0 \ll \phi_0$. Our criterion will be the following: For the same dimensionless ridge curvature $\tilde{\Lambda}_\phi$ and the same initial proximity to the ridge θ_0 , the strength of the attractor is defined through the number of efolds $N \leq 60$ it takes for the inflaton field to develop a large angle in field space, $\theta \simeq 1$.

Following the linearized analysis of [36], we take the dominant field ϕ to follow the single-field slow-roll solution, which is consistent to linear order in χ

$$\dot{\phi}_{\text{SR}} = -\frac{\sqrt{\lambda_\phi} M_{\text{pl}}^3}{3\sqrt{3}\xi_\phi^2 \phi} \quad (33)$$

which can be trivially solved to give

$$\phi = \sqrt{\phi_0^2 - \frac{4}{3} \frac{M_{\text{pl}}^2}{\xi_\phi} N} \quad (34)$$

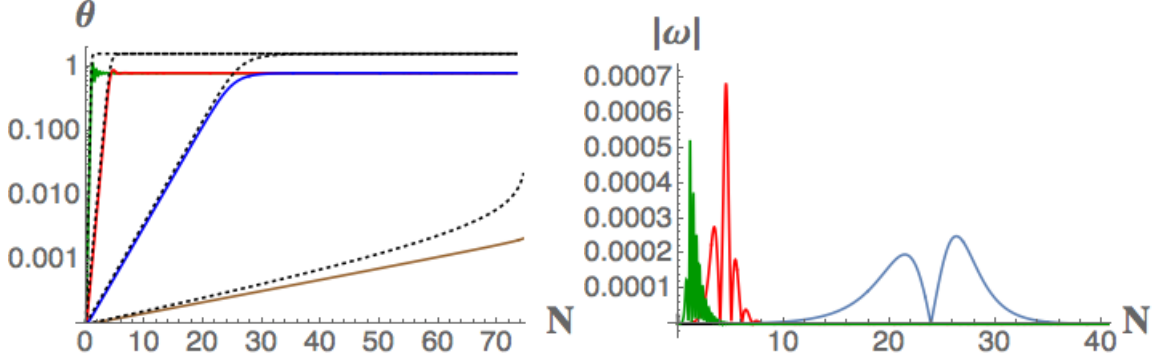


FIG. 4: (*Left*) Evolution of the angle θ as a function of number of e-folds from the beginning of inflation for $\tilde{\Lambda}_\phi = 0.001$, $\theta_0 = 10^{-4}$, $\xi_\chi = \xi_\phi$ and $\lambda_\phi = \lambda_\chi$. The values of the nonminimal coupling are $\xi_\phi = 10, 10^2, 10^3, 10^4$ (brown, blue, red, and green respectively). The black dotted lines show the analytic results from Eq. (38). (*Right*) Evolution of the turn rate $|\omega| \equiv |\omega^I|$ as a function of the number of e-folds from the beginning of inflation for the same parameters and color-coding. The turn-rate for $\xi_\phi = 10$ is too small ($|\omega| \lesssim 10^{-7}$) to be visible on this plot.

where $\phi(N=0) = \phi_0$ at the start of inflation and we take the Hubble term to be constant

$$H \simeq \sqrt{\frac{\lambda_\phi}{12\xi_\phi^2}} M_{\text{pl}}. \quad (35)$$

The linearized equation of motion for the secondary field χ , when starting near the top of a smooth ridge ($\theta_0 \ll 1, \tilde{\Lambda}_\phi \ll 1$) is

$$\ddot{\chi} + 3H\dot{\chi} - \frac{\tilde{\Lambda}_\phi M_{\text{pl}}^2}{\xi_\phi} \chi = 0 \quad (36)$$

where the solution (for $H = \text{const.}$) is

$$\chi(N) \simeq \chi_0 \exp \left[\left(-\frac{3}{2} + \sqrt{\frac{9}{4} + 12\tilde{\Lambda}_\phi \xi_\phi} \right) N \right]. \quad (37)$$

The evolution of the field-space angle θ follows immediately as

$$\theta(N) = \arctan \left(\frac{\exp \left[\left(-\frac{3}{2} + \sqrt{\frac{9}{4} + 12\tilde{\Lambda}_\phi \xi_\phi} \right) N \right]}{\theta_0 \sqrt{1 - \frac{4}{3} \frac{M_{\text{pl}}^2}{\xi_\phi \phi_0^2} N}} \right). \quad (38)$$

As we can easily see from Fig. 4, for the same amount of fine-tuning $\tilde{\Lambda}_\phi$ and initial position θ_0 , the attractor gets stronger as ξ_ϕ increases. We only consider this fine-tuned regime, since for $\tilde{\Lambda} = \mathcal{O}(1)$ or $\theta_0 = \mathcal{O}(1)$, the approach to the attractor is too fast for the extraction of any reasonable conclusion. In Fig. 4 we also plot the turn-rate $|\omega| \equiv |\omega^I|$ as a function of time. For $\xi_\phi = 10$ and fine-tuned initial conditions, the attractor is too weak and the field remains on the ridge for the duration of the inflationary epoch, leading to a suppressed turn-rate $|\omega| \lesssim 10^{-7}$. For larger

values of ξ_ϕ we see that the turn-rate spikes at the time when $\theta \simeq 1$, as expected. The turn-rate spikes earlier for larger couplings, indicating again a stronger attractor behavior. In the cases of $\xi_\phi = 10^3, 10^4$, the attractor is strong enough (meaning that the ridge is steep enough) that the field reaches the valley of the potential while having a significant velocity, which leads to it oscillate around the minimum before settling down to single-field motion. These oscillations perpendicular to the dominant motion of the inflaton can be seen as “primordial clocks” with possibly interesting observational consequences [86–89].

Inflation ends when the scale factor stops accelerating, $\ddot{a}(t_{\text{end}}) = 0$, which is equivalent to $\epsilon(t_{\text{end}}) = 1$. After t_{end} , the background fields $\varphi^I(t)$ oscillate around the global minimum of the potential, governed by Eq. (15). If (as is generic) the system settles into the single-field attractor before the end of inflation, then the motion of $\varphi^I(t)$ in the direction of the potential’s valley remains suppressed even after inflation. For example, if the system evolves along a valley in the $\chi = 0$ direction during inflation, then $\chi \sim \dot{\chi} \sim 0$ at t_{end} and Eq. (15) will maintain $\chi \sim \dot{\chi} \sim 0$ for times $t > t_{\text{end}}$, as shown in Fig. 5. (Such attractor behavior after t_{end} will persist for at least as long as backreaction from perturbations may be neglected, consistent with the linearized treatment of Eq. (10).) Thus the strong attractor behavior that was identified in [33–36] is characteristic of the preheating phase as well.

The persistence of the attractor behavior after the end of inflation has important implications for preheating. In particular, although the unit vectors $\hat{\sigma}^I$ and \hat{s}^I may become ill-defined when the motion of $\varphi^I(t)$ is no longer monotonic, the orientation of the attractor in field space, $\theta = \arctan(\chi/\phi)$, remains unchanged after inflation. Upon performing a rotation $\varphi^I \rightarrow \varphi^{I'}$ such that $\chi' = 0$ lies along the direction of the attractor, then only one field, $\phi'(t)$, oscillates after t_{end} . With only one background field oscillating, there is no “de-phasing” of the background fields’ oscillations, as is typical for multifield models with minimal couplings [21, 52, 53]. As we will see in Section IV, these attractor models therefore predict robust, resonant amplification of fluctuations.

Within a single-field attractor, both the field-space metric, \mathcal{G}_{IJ} , and the mass-squared tensor, \mathcal{M}_{IJ} of Eq. (18), become effectively diagonal. Upon rotating $\varphi^I \rightarrow \varphi^{I'}$ as needed so that the attractor lies along the direction $\chi' = 0$, then $\mathcal{G}_{\phi'\chi'} \sim \mathcal{G}^{\phi'\chi'} \sim 0$ and $\mathcal{M}_{\chi'}^{\phi'} \sim \mathcal{M}_{\phi'}^{\chi'} \sim 0$. As we will see in Section IV, this feature greatly simplifies the analysis of the fluctuations. Given that we may always perform such a field-space rotation, for most of the following analysis we restrict attention to cases in which the attractor lies along the direction $\chi = 0$ with no loss of generality. In Section IV C we demonstrate that our results remain robust even for cases in which the attractor lies along some other direction θ in field space.

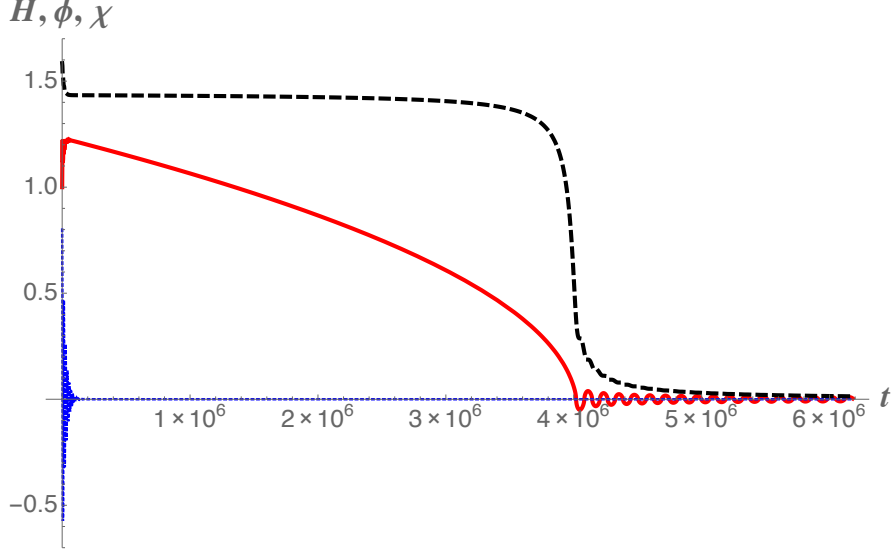


FIG. 5: The evolution of $H(t)$ (black dashed line), $\phi(t)$ (red solid line), and $\chi(t)$ (blue dotted line) during and after inflation, in units of M_{pl} . The evolution shown here is for $\xi_\chi = 0.8 \xi_\phi$, $\lambda_\chi = 1.25 \lambda_\phi$, and $g = \lambda_\phi$, with $\xi_\phi = 10^2$, $\lambda_\phi = 10^{-4}$, and initial conditions $\phi(t_0) = 1$, $\chi(t_0) = 0.8$, $\dot{\phi}(t_0) = \dot{\chi}(t_0) = 0$. (We plot $5 \times 10^4 H$ so its magnitude is comparable to ϕ .) With these parameters and initial conditions, inflation lasts for $N_{\text{tot}} = 111.6$ efolds until $t_{\text{end}} = 3.99 \times 10^6$. The system rapidly falls into a valley along $\chi = 0$ within the first 3 efolds of inflation, after which $\chi(t)$ remains fixed at $\chi \sim 0$. After t_{end} , $\phi(t)$ oscillates around the global minimum of the potential.

B. End of Inflation and Effective Equation of State

Within the single-field attractor, we may readily study how $\phi(t_{\text{end}})$ depends on the coupling constants. First we note that in the single-field attractor (assumed to lie along a $\chi = 0$ valley), the evolution of $\phi(t)$ becomes independent of λ_χ , g , and ξ_χ . Furthermore, we may rescale $t \rightarrow \tau \equiv \sqrt{\lambda_\phi} t$ without affecting the dynamics: $N = \int H dt = \int \mathcal{H} d\tau$ remains unchanged, as does $\epsilon = -\mathcal{H}'/\mathcal{H}^2 = -\dot{H}/H^2$ (where $\mathcal{H} \equiv a'/a$ and primes denote $d/d\tau$). Therefore $\phi(\tau_{\text{end}}) = \phi(t_{\text{end}})$. Thus in the single-field attractor, the value of ϕ at the end of inflation depends only on ξ_ϕ . In the limit $\xi_\phi \gg 1$, we expect inflation to end when $\xi_\phi \phi^2(t_{\text{end}}) \simeq M_{\text{pl}}^2$, which is indeed the behavior we observe. As shown in Fig. 6, $\phi(t_{\text{end}})$ is very well fit by $\phi(t_{\text{end}}) = 0.8 M_{\text{pl}}/\sqrt{\xi_\phi}$ for $\xi_\phi \geq 1$, whereas $\phi(t_{\text{end}}) \rightarrow 2.1 M_{\text{pl}}$ in the limit $\xi_\phi \ll 1$, approaching the result of a minimally coupled ϕ^4 model. The value $\phi(t_{\text{end}})$ sets the initial amplitude of oscillations at the start of preheating.

We may estimate the effective equation of state during the preheating phase by using the virial theorem [90]. The total kinetic energy for the system (to background order) is [33]

$$\frac{1}{2} \dot{\sigma}^2 \equiv \frac{1}{2} \mathcal{G}_{IJ} \dot{\phi}^I \dot{\phi}^J, \quad (39)$$

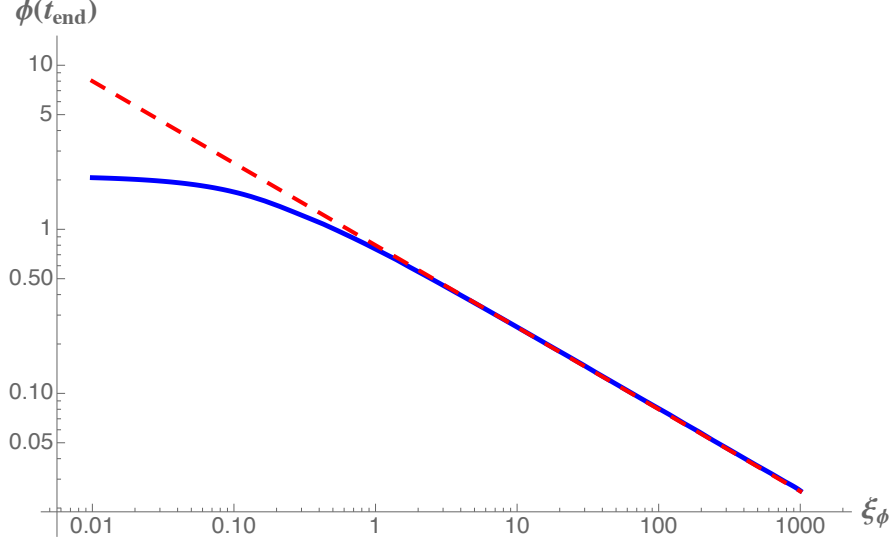


FIG. 6: Within the single-field attractor, the value of $\phi(t_{\text{end}})$ depends only on ξ_ϕ . The blue curve shows the numerical evaluation of $\phi(t_{\text{end}})$ (in units of M_{pl}), while the red dashed curve shows $0.8/\sqrt{\xi_\phi}$.

and the energy density and pressure are given by

$$\begin{aligned}\rho &= \frac{1}{2}\dot{\sigma}^2 + V(\varphi^I), \\ p &= \frac{1}{2}\dot{\sigma}^2 - V(\varphi^I).\end{aligned}\tag{40}$$

If we assume an equation of state of the form $p = w\rho$, then we find

$$w = \frac{\dot{\sigma}^2 - 2V}{\dot{\sigma}^2 + 2V}\tag{41}$$

to background order. Using Eqs. (16), (39), and (40), we may rewrite Eq. (22) as $\epsilon = 3\dot{\sigma}^2/(\dot{\sigma}^2 + 2V)$. At t_{end} , before the oscillations have begun, we have $\epsilon = 1$ and therefore $w = -1/3$, independent of couplings.

To estimate w once the background fields begin to oscillate, we define a covariant expression for the virial, q ,

$$q \equiv \mathcal{G}_{IJ}\dot{\varphi}^I\varphi^J.\tag{42}$$

Upon using $\partial\mathcal{G}_{IJ}/\partial t = (\partial_K\mathcal{G}_{IJ})\dot{\varphi}^K$ and the usual relations among the Christoffel symbols Γ_{JK}^I , we find

$$\dot{q} = \dot{\sigma}^2 - V_{,J}\varphi^J + \frac{1}{2}(\partial_K\mathcal{G}_{IJ})\dot{\varphi}^I\dot{\varphi}^J\varphi^K.\tag{43}$$

Eq. (43) is analogous to applications of the virial theorem in general relativity, in which corrections to the Newtonian result enter as gradients of the metric components [91]. For trajectories within

the single-field attractor (with $\chi \sim \dot{\chi} \sim 0$), we have $\dot{\sigma}^2 \simeq \mathcal{G}_{\phi\phi}\dot{\phi}^2$ and Eq. (43) becomes

$$\dot{q} \simeq \dot{\sigma}^2 \left[1 + \frac{1}{2} \phi \partial_\phi \ln \mathcal{G}_{\phi\phi} \right] - V_{,J} \varphi^J. \quad (44)$$

From Eqs. (4) and (20), we further find

$$V_{,J} \varphi^J = 2M_{\text{pl}}^2 \frac{V}{f}, \quad (45)$$

where f is the nonminimal-coupling function of Eq. (19). Upon time-averaging over several oscillations we have $\langle \dot{q} \rangle = 0$, and hence

$$\langle \dot{\sigma}^2 \rangle + \frac{1}{2} \langle \dot{\sigma}^2 \cdot \phi \partial_\phi \ln \mathcal{G}_{\phi\phi} \rangle = 2M_{\text{pl}}^2 \langle V/f \rangle \quad (46)$$

where the second term on the left-hand side is the contribution of the stretched field-space manifold. The equation of state can be calculated by noting that energy conservation requires (if one neglects Hubble friction)

$$\dot{\sigma}^2 + 2V = 2V_{\text{max}} \quad (47)$$

which allows for Eq. (41) to be written solely in terms of ϕ and not $\dot{\phi}$.

After t_{end} , $\phi(t)$ begins to oscillate with an initial amplitude $\phi(t_{\text{end}}) \sim M_{\text{pl}}/\sqrt{\xi_\phi}$ for $\xi_\phi \gtrsim 1$; at later times, its amplitude falls due to both the expansion of the universe and the transfer of energy to decay products. Fig. 7 shows the equation of state w_{avg} calculated by solving the background evolution and averaging Eq. (41) over several oscillations of $\phi(t)$, starting at the end of inflation, where $w = -1/3$. We see that for large nonminimal couplings, the equation of state spends more time around $\bar{w} \approx 0$, as the universe continues to expand, while eventually reaching $\bar{w} = 1/3$ at late times. Early in the oscillation phase, in other words, the conformal stretching of the Einstein-frame potential makes the background field behave more like a minimally coupled field in a quadratic potential, $V(\phi) = \frac{1}{2}m^2\phi^2$, than a quartic potential, $V(\phi) = \frac{\lambda}{4}\phi^4$. At late times, however, the system behaves like radiation, as in the minimally coupled case. Across the range $10^{-1} \leq \xi_\phi \leq 10^2$, w_{avg} reaches $1/3$ within a few efolds after the end of inflation.

C. Background-Field Oscillations

To facilitate comparison with the well-studied case of a minimally coupled field with quartic self-coupling, in this subsection we neglect Hubble expansion during the oscillating phase. This approximation becomes more reliable as the frequency of oscillation ω grows significantly larger

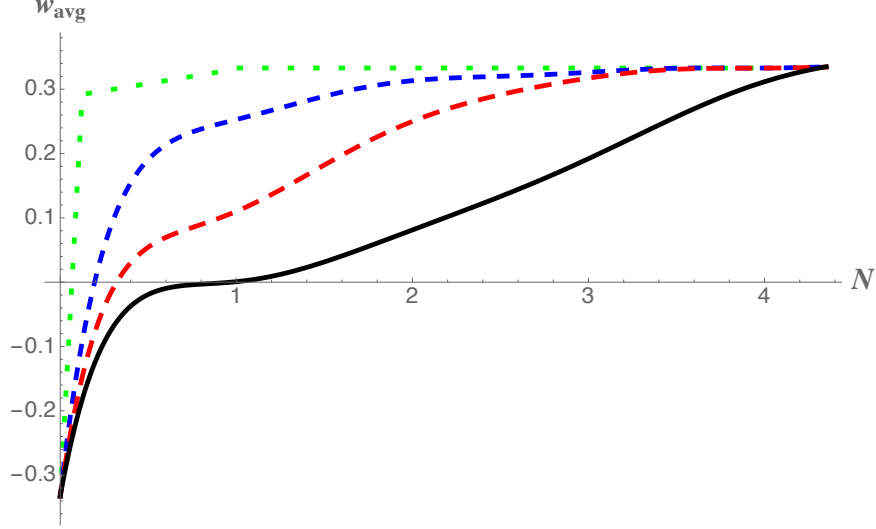


FIG. 7: The equation of state, w from Eq. (41), averaged over several oscillations of $\phi(t)$, as a function of e-folds, N , after the end of inflation. From bottom to top: $\xi_\phi = 100$ (black line), $\xi_\phi = 10$ (red dashed line), $\xi_\phi = 1$ (blue short-dashed line), and $\xi_\phi = 0.1$ (green dotted line). All simulations used $\xi_\chi = 0.8 \xi_\phi$, $\lambda_\chi = 1.25 \lambda_\phi$, and $g = \lambda_\phi$. Initial conditions at the start of inflation were set as $\theta_0 = \arctan(\chi_0/\phi_0) = \pi/6$; in each case, the fields settled into the single-field attractor along $\chi \sim 0$ before the end of inflation.

than H ; in our case, we find a modest separation of time-scales, with $\omega/H > 1$ across a wide range of ξ_ϕ . (One may incorporate effects from the expansion of the universe perturbatively [92], though the $H \sim 0$ limit will suffice for our purposes here.)

Within the single-field attractor, in the limit $H \rightarrow 0$ and neglecting backreaction from produced particles, Eq. (15) becomes

$$\ddot{\phi} + \Gamma_{\phi\phi}^{\phi} \dot{\phi}^2 + \mathcal{G}^{\phi\phi} V_{,\phi} \simeq 0. \quad (48)$$

We rescale $\tau \equiv \sqrt{\lambda_\phi} t$, so that the dynamics depend only on ξ_ϕ . After τ_{end} , $\phi(\tau)$ oscillates periodically with period given by

$$T = 2 \int_{-\phi_0}^{\phi_0} d\phi \sqrt{\frac{\mathcal{G}_{\phi\phi}}{2V(\phi_0) - 2V(\phi)}}. \quad (49)$$

(In this subsection we label $\phi_0 = \phi(\tau_{\text{end}})$ as the amplitude of the field at the start of preheating, rather than the start of inflation.) As shown in Fig. 8, the period scales approximately linearly with ξ_ϕ for $\xi_\phi > 1$, and hence the frequency of oscillations, $\omega = 2\pi/T$, scales like $1/\xi_\phi$. The Hubble scale at the end of inflation, $H(t_{\text{end}})$, also scales like $1/\xi_\phi$ in the limit of large ξ_ϕ . We find $\omega/H(t_{\text{end}}) > 1$ across the entire range $10^{-3} \leq \xi_\phi \leq 10^3$, with $\omega/H(t_{\text{end}}) \sim 3$ at $\xi_\phi = 1$ and $\omega/H(t_{\text{end}}) \rightarrow 4$ for $\xi_\phi \gg 1$.

In the limit $\xi_\phi \gg 1$, the integral for T in Eq. (49) may be calculated analytically. For initial data of the form $\phi_0 = \phi(\tau_{\text{end}}) = \alpha M_{\text{pl}}/\sqrt{\xi_\phi}$ for some constant α (e.g., $\alpha = 0.8$ as above), and

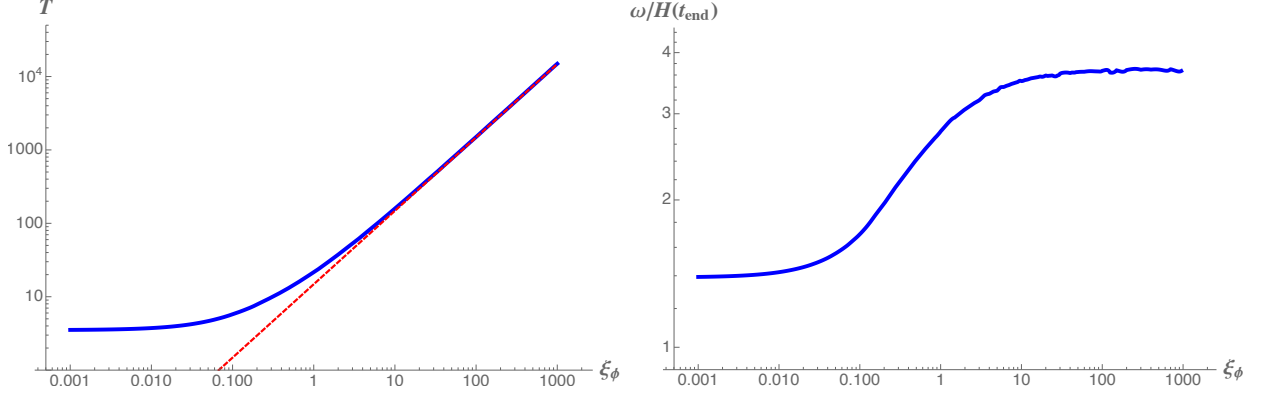


FIG. 8: (*Left*) The period of $\phi(\tau)$'s oscillations, T (in units of M_{pl}), as a function of ξ_ϕ , within the single-field attractor. For large ξ_ϕ , T grows linearly with ξ_ϕ , asymptoting to $T \rightarrow 14.8\xi_\phi/M_{\text{pl}}$ (red dashed line). (*Right*) The ratio of the frequency of ϕ 's oscillations, $\omega = 2\pi/T$, to the Hubble scale at the end of inflation, $H(t_{\text{end}})$. For large ξ_ϕ , both ω and $H(t_{\text{end}})$ scale as $1/\xi_\phi$, with $\omega/H(t_{\text{end}}) > 1$.

working in the regime $\alpha > 1/\sqrt{6\xi_\phi}$, we find

$$T \rightarrow \frac{4\sqrt{3}\xi_\phi}{M_{\text{pl}}} \left[\pi - \arctan \left(\frac{\sqrt{1+2\alpha^2}}{\alpha^2} \right) \right] \frac{1+\alpha^2}{\sqrt{1+2\alpha^2}}. \quad (50)$$

Details of this derivation are found in Appendix B. Using the best-fit value $\alpha = 0.8$ (see Fig. 6) yields $T \rightarrow 14.8\xi_\phi/M_{\text{pl}}$ in the limit $\xi_\phi \gg 1$. Meanwhile, in the opposite limit, $\xi_\phi \rightarrow 0$, Eq. (48) may be solved analytically as a Jacobian elliptic cosine, given the Jordan-frame potential of Eq. (20): $\phi(t) = \phi_0 \text{cn}(\phi_0\tau, 1/\sqrt{2})$ [93–95]. The function $\text{cn}(x, \kappa)$ is periodic with period $4K(\kappa)$, where $K(\kappa)$ is the complete elliptic integral of the first kind [96]. Given $\kappa = 1/\sqrt{2}$ and $\phi_0 = 2.1 M_{\text{pl}}$ for $\xi_\phi = 0$, we find $T \rightarrow 4K(1/\sqrt{2})/\phi_0 = 3.9/M_{\text{pl}}$, a good match to the $\xi_\phi \ll 1$ behavior of Fig. 8.

More generally, the terms in Eq. (48) that arise from the nontrivial field-space metric produce a richer structure for ϕ 's oscillations, with greater numbers of non-negligible harmonics, compared to the $\xi_\phi = 0$ case. In [51] we study this nontrivial harmonic structure and analyze its impact on the structure of the resonances for the coupled fluctuations.

IV. EVOLUTION OF THE FLUCTUATIONS

In order to study the evolution of the fluctuations Q^I during preheating, we expand the action to second order in both field and metric perturbations, calculate the energy density, and perform a (covariant) mode expansion. These steps enable us to relate the number density of particles for each species to an adiabatic parameter, generalizing the usual single-field expression. Using the adiabatic parameters, we identify regions of parameter space in which the system departs strongly

from adiabatic evolution, indicating explosive particle production. We find important differences in the behavior of these resonances in the limits $\xi_\phi \gg 1$ and $\xi_\phi < 1$.

A. Mode Expansion and Adiabatic Parameters

Following the method of [71] applied to the action in Eq. (3), we may expand the action to second order in the doubly-covariant fluctuation Q^I . We find (see also [33, 54, 69])

$$S_2^{(Q)} = \int d^3x dt a^3(t) \left[-\frac{1}{2} \bar{g}^{\mu\nu} \mathcal{G}_{IJ} \mathcal{D}_\mu Q^I \mathcal{D}_\nu Q^J - \frac{1}{2} \mathcal{M}_{IJ} Q^I Q^J \right], \quad (51)$$

where $\bar{g}_{\mu\nu}$ is the background spacetime metric, \mathcal{M}_{IJ} is given in Eq. (18), and \mathcal{G}_{IJ} and \mathcal{M}_{IJ} are evaluated to background order in the fields, φ^I . Next we rescale the fluctuations, $Q^I(x^\mu) \rightarrow X^I(x^\mu)/a(t)$ and introduce conformal time, $d\eta = dt/a(t)$, so that the background spacetime line-element may be written $ds^2 = a^2(\eta) \eta_{\mu\nu} dx^\mu dx^\nu$, in terms of the Minkowski spacetime metric $\eta_{\mu\nu}$. Upon integrating by parts, we may rewrite Eq. (51) in the form

$$S_2^{(X)} = \int d^3x d\eta \left[-\frac{1}{2} \eta^{\mu\nu} \mathcal{G}_{IJ} \mathcal{D}_\mu X^I \mathcal{D}_\nu X^J - \frac{1}{2} \mathbb{M}_{IJ} X^I X^J \right] \quad (52)$$

where

$$\mathbb{M}_{IJ} \equiv a^2 \left(\mathcal{M}_{IJ} - \frac{1}{6} \mathcal{G}_{IJ} R \right) \quad (53)$$

and R is the spacetime Ricci scalar. We have used the relation $R = 6a''/a^3$, and in this section we will use primes to denote $d/d\eta$. Note that for an equation of state $w_{\text{avg}} \simeq 0$ then $a(t) \sim t^{2/3}$ and $a(\eta) \sim \eta^2$, while for $w_{\text{avg}} = 1/3$ then $a(t) \sim t^{1/2}$ and $a(\eta) \sim \eta$.

From Eq. (52) we may construct an energy-momentum tensor for the fluctuations,

$$T_{\mu\nu}^{(X)} = \mathcal{G}_{IJ} \mathcal{D}_\mu X^I \mathcal{D}_\nu X^J - \frac{1}{2} \eta_{\mu\nu} \left[\eta^{\alpha\beta} \mathcal{G}_{IJ} \mathcal{D}_\alpha X^I \mathcal{D}_\beta X^J + \mathbb{M}_{IJ} X^I X^J \right]. \quad (54)$$

The energy density is given by the 00 component of $T_{\mu\nu}^{(X)}$. The background spacetime metric is spatially flat, so we may easily perform a Fourier transform of a given quantity, $F(x^\mu) = (2\pi)^{-3/2} \int d^3k F_k(\eta) e^{i\mathbf{k}\cdot\mathbf{x}}$. The energy density of the fluctuations per Fourier mode then takes the form

$$\rho_k^{(X)} = \frac{1}{2} \mathcal{G}_{IJ} \mathcal{D}_\eta X_k^I \mathcal{D}_\eta X_k^J + \frac{1}{2} [\omega_k^2(\eta)]_{IJ} X_k^I X_k^J + \mathcal{O}(X^3), \quad (55)$$

where we have defined

$$[\omega_k^2(\eta)]_{IJ} \equiv k^2 \mathcal{G}_{IJ} + \mathbb{M}_{IJ}. \quad (56)$$

Upon using the equation of motion for Q^I , Eq. (17), and the relation $Q^I = X^I/a$, we may rewrite Eq. (55) in the form

$$\rho_k^{(X)} = \frac{1}{2} \mathcal{G}_{IJ} [(\mathcal{D}_\eta X^I) (\mathcal{D}_\eta X^J) - (\mathcal{D}_\eta^2 X^I) X^J]. \quad (57)$$

Next we quantize the fluctuations, $X^I \rightarrow \hat{X}^I$, and expand them in a series of creation and annihilation operators in a way that respects the nontrivial field-space manifold [21, 97],

$$\hat{X}^I(x^\mu) = \int \frac{d^3k}{(2\pi)^{3/2}} \sum_b \left[u_b^I(k, \eta) \hat{a}_{\mathbf{k}b} e^{i\mathbf{k}\cdot\mathbf{x}} + u_b^{I*}(k, \eta) \hat{a}_{\mathbf{k}b}^\dagger e^{-i\mathbf{k}\cdot\mathbf{x}} \right], \quad (58)$$

where the index $b = 1, 2, \dots, N$. The operators obey

$$\hat{a}_{\mathbf{k}b}|0\rangle = 0, \quad \langle 0|\hat{a}_{\mathbf{k}b}^\dagger = 0 \quad (59)$$

for all \mathbf{k} and b , and

$$\begin{aligned} [\hat{a}_{\mathbf{k}b}, \hat{a}_{\mathbf{q}c}] &= [\hat{a}_{\mathbf{k}b}^\dagger, \hat{a}_{\mathbf{q}c}^\dagger] = 0, \\ [\hat{a}_{\mathbf{k}b}, \hat{a}_{\mathbf{q}c}^\dagger] &= \delta^{(3)}(\mathbf{k} - \mathbf{q}) \delta_{bc}. \end{aligned} \quad (60)$$

Each of the mode functions satisfies the equation of motion,

$$\mathcal{D}_\eta^2 u_b^I + [\omega_k^2(\eta)]_J^I u_b^J = 0. \quad (61)$$

As discussed in [21], we have N linear, second-order differential equations (one for each \hat{X}^I), which yield $2N$ linearly independent solutions. By parameterizing the fluctuations as in Eq. (58), we have introduced N^2 complex mode functions $u_b^I(k, \eta)$, and hence $2N^2$ real-valued scalar functions, $u_b^I = \text{Re}[u_b^I] + \text{Im}[u_b^I]$. But N -tuples of the complex mode functions are coupled to each other by Eq. (61), which yields $2N(N-1)$ constraints, leaving exactly $2N^2 - 2N(N-1) = 2N$ independent solutions.

We parameterize the mode functions as [21, 97]

$$u_b^I(k, \eta) = h_{(b,I)}(k, \eta) e_b^I(\eta), \quad (62)$$

where the $h_{(b,I)}$ are complex scalar functions and the $e_b^I(\eta)$ are vielbeins of the field-space metric,

$$\delta^{bc} e_b^I(\eta) e_c^J(\eta) = \mathcal{G}^{IJ}(\eta). \quad (63)$$

Note that the components of the vielbeins are purely real, and, unlike the unit vectors $\hat{\sigma}^I, \hat{s}^I$ defined in Eq. (30), the e_b^I are well-behaved during preheating. (Explicit expressions for the e_b^I for our

two-field model may be found in Appendix A.) The subscripts (b, I) on h are labels only, not vector indices. We then find

$$\langle 0 | \hat{X}^I(x) \hat{X}^J(x) | 0 \rangle = \int \frac{d^3 k}{(2\pi)^3} \delta^{bc} u_b^I u_c^{J*}, \quad (64)$$

upon using Eqs. (59), (60), and (63). As emphasized in [21, 24], the cross products, with $I \neq J$, need not vanish.

The vielbeins “absorb” most of the added structure from the nontrivial field-space manifold, enabling us to manipulate (mostly) ordinary scalar functions. As usual, we raise and lower field-space indices I, J with \mathcal{G}_{IJ} , and we raise and lower internal indices b, c with δ_{bc} . We may also use the vielbeins to “trade” between field-space indices and internal indices. For an arbitrary vector A^I we may write

$$A^b = e^b_I A^I, \quad A^I = e^I_b A^b, \quad (65)$$

while Eq. (63) implies

$$\begin{aligned} e^b_I e^I_c &= \delta^b_c, \\ e^I_b e^b_J &= \delta^I_J. \end{aligned} \quad (66)$$

The covariant derivative of the vielbein with respect to \mathcal{G}_{IJ} is given in terms of the spin connection, ω^{bc}_I ,

$$\mathcal{D}_I e^b_J = -\omega^{bc}_I e_{cJ}, \quad (67)$$

where ω^{bc}_I is antisymmetric in its internal indices, $\omega^{bc}_I = -\omega^{cb}_I$ [98]. Because of the antisymmetry of the spin connection, the (covariant) directional derivative with respect to conformal time vanishes,

$$\mathcal{D}_\eta e^b_J = 0 \quad (68)$$

for all b and J [97].

For our two-field model, with $\{I, J\} = \{1, 2\}$, we may write out the mode expansions more explicitly. We assign the field-space indices $1 = \phi$ and $2 = \chi$ and write $\hat{a}_{\mathbf{k}b} = \hat{b}_{\mathbf{k}}$ for $b = 1$, $\hat{a}_{\mathbf{k}b} = \hat{c}_{\mathbf{k}}$ for $b = 2$. We also label $h_{(1,\phi)} = v_k(\eta)$, $h_{(2,\phi)} = w_k(\eta)$, $h_{(1,\chi)} = y_k(\eta)$, and $h_{(2,\chi)} = z_k(\eta)$, so that Eq. (58) becomes

$$\begin{aligned} \hat{X}^\phi(x^\mu) &= \int \frac{d^3 k}{(2\pi)^{3/2}} \left[\left(v_k e_1^\phi \hat{b}_{\mathbf{k}} + w_k e_2^\phi \hat{c}_{\mathbf{k}} \right) e^{i\mathbf{k} \cdot \mathbf{x}} + \left(v_k^* e_1^\phi \hat{b}_{\mathbf{k}}^\dagger + w_k^* e_2^\phi \hat{c}_{\mathbf{k}}^\dagger \right) e^{-i\mathbf{k} \cdot \mathbf{x}} \right], \\ \hat{X}^\chi(x^\mu) &= \int \frac{d^3 k}{(2\pi)^{3/2}} \left[\left(y_k e_1^\chi \hat{b}_{\mathbf{k}} + z_k e_2^\chi \hat{c}_{\mathbf{k}} \right) e^{i\mathbf{k} \cdot \mathbf{x}} + \left(y_k^* e_1^\chi \hat{b}_{\mathbf{k}}^\dagger + z_k^* e_2^\chi \hat{c}_{\mathbf{k}}^\dagger \right) e^{-i\mathbf{k} \cdot \mathbf{x}} \right]. \end{aligned} \quad (69)$$

Eq. (61) couples v_k with y_k and w_k with z_k :

$$\begin{aligned}
\left(v_k'' + \Omega_{(\phi)}^2 v_k\right) e_1^\phi &= -a^2 \mathcal{M}_\chi^\phi y_k e_1^\chi, \\
\left(w_k'' + \Omega_{(\phi)}^2 w_k\right) e_2^\phi &= -a^2 \mathcal{M}_\chi^\phi z_k e_2^\chi, \\
\left(y_k'' + \Omega_{(\chi)}^2 y_k\right) e_1^\chi &= -a^2 \mathcal{M}_\phi^\chi v_k e_1^\phi, \\
\left(z_k'' + \Omega_{(\chi)}^2 z_k\right) e_2^\chi &= -a^2 \mathcal{M}_\phi^\chi w_k e_2^\phi,
\end{aligned} \tag{70}$$

where for convenience we have labeled the diagonal components of $[\omega_k^2(\eta)]^I_J$ as

$$\begin{aligned}
\Omega_{(\phi)}^2(k, \eta) &\equiv k^2 + a^2 m_{\text{eff}, \phi}^2(\eta), \\
\Omega_{(\chi)}^2(k, \eta) &\equiv k^2 + a^2 m_{\text{eff}, \chi}^2(\eta),
\end{aligned} \tag{71}$$

in terms of the effective masses

$$\begin{aligned}
m_{\text{eff}, \phi}^2 &\equiv \mathcal{M}_\phi^\phi - \frac{1}{6}R, \\
m_{\text{eff}, \chi}^2 &\equiv \mathcal{M}_\chi^\chi - \frac{1}{6}R.
\end{aligned} \tag{72}$$

We are interested in the energy density per mode k of the quantized fluctuations, which we parameterize as

$$\langle \hat{\rho}^{(X)}(x^\mu) \rangle = \int \frac{d^3 k}{(2\pi)^3} \rho_k^{(X)\text{vev}}(\eta). \tag{73}$$

Upon using Eqs. (57), (64), and (68) we find

$$\begin{aligned}
\rho_k^{(X)\text{vev}} &= \frac{1}{2} \mathcal{G}_{IJ} \sum_b \sum_c \left\{ \delta^{bc} \left[h'_{(b,I)} h_{(c,J)}^{*'} - h''_{(b,I)} h_{(c,J)}^* \right] e_b^I e_c^J \right\} \\
&= \rho_k^{(\phi)} + \rho_k^{(\chi)} + \rho_k^{(\text{int})},
\end{aligned} \tag{74}$$

with

$$\begin{aligned}
\rho_k^{(\phi)} &= \frac{1}{2} \mathcal{G}_{\phi\phi} \left\{ (|v_k'|^2 - v_k'' v_k^*) e_1^\phi e_1^\phi + (|w_k'|^2 - w_k'' w_k^*) e_2^\phi e_2^\phi \right\}, \\
\rho_k^{(\chi)} &= \frac{1}{2} \mathcal{G}_{\chi\chi} \left\{ (|y_k'|^2 - y_k'' y_k^*) e_1^\chi e_1^\chi + (|z_k'|^2 - z_k'' z_k^*) e_2^\chi e_2^\chi \right\} \\
\rho_k^{(\text{int})} &= \mathcal{G}_{\phi\chi} \left\{ (v_k' y_k^{*'} - v_k'' y_k^*) e_1^\phi e_1^\chi + (y_k' v_k^{*'} - y_k'' v_k^*) e_1^\chi e_1^\phi \right. \\
&\quad \left. + (w_k' z_k^{*'} - w_k'' z_k^*) e_2^\phi e_2^\chi + (z_k' w_k^{*'} - z_k'' w_k^*) e_2^\chi e_2^\phi \right\}.
\end{aligned} \tag{75}$$

One may use the equations of motion in Eq. (70) to demonstrate that the expressions in Eq. (75) are purely real. The number density per mode of quanta of a given field I (ϕ or χ) may be related to the energy density by

$$n_k^{(I)} = \frac{\rho_k^{(I)}}{\Omega_{(I)}} - \frac{1}{2}. \tag{76}$$

The number density per mode for each species $I = \phi, \chi$ will be well-defined in the limit $\rho_k^{(\text{int})} \ll \rho_k^{(I)}$.

We noted in Section III A that within a single-field attractor (along the direction $\chi = 0$), the cross-terms in both \mathcal{G}_{IJ} and \mathcal{M}_J^I vanish. In that case, the vielbeins also become diagonal,

$$e_b^I \rightarrow \begin{pmatrix} e_1^\phi & 0 \\ 0 & e_2^\chi \end{pmatrix}, \quad (77)$$

with $e_2^\phi \sim e_1^\chi \sim 0$, $e_1^\phi e_1^\phi \simeq \mathcal{G}^{\phi\phi}$, $e_2^\chi e_2^\chi \simeq \mathcal{G}^{\chi\chi}$, and $\mathcal{G}_{\phi\phi} \mathcal{G}^{\phi\phi} = \mathcal{G}_{\chi\chi} \mathcal{G}^{\chi\chi} = 1 + \mathcal{O}(\chi^2)$. Then the fluctuations \hat{X}^I simplify considerably: \hat{X}^ϕ is expanded only in the $\hat{b}_{\mathbf{k}}, \hat{b}_{\mathbf{k}}^\dagger$ operators, and \hat{X}^χ only in the $\hat{c}_{\mathbf{k}}, \hat{c}_{\mathbf{k}}^\dagger$ operators. Given both $\mathcal{M}_\chi^\phi \sim \mathcal{M}_\phi^\chi \sim 0$ and $e_2^\phi \sim e_1^\chi \sim 0$, moreover, the scalar mode functions decouple: the functions $v_k(\eta)$ and $z_k(\eta)$ satisfy source-free equations of motion, while $w_k(\eta) \sim y_k(\eta) \sim 0$. Within the attractor, the expressions in Eq. (75) simplify as well:

$$\begin{aligned} \rho_k^{(\phi)} &\rightarrow \frac{1}{2} (|v_k'|^2 - v_k'' v_k^*) + \mathcal{O}(\chi^2), \\ \rho_k^{(\chi)} &\rightarrow \frac{1}{2} (|z_k'|^2 - z_k'' z_k^*) + \mathcal{O}(\chi^2), \\ \rho_k^{(\text{int})} &\rightarrow \mathcal{O}(\chi^2) \sim 0. \end{aligned} \quad (78)$$

Since $\rho_k^{(\text{int})}$ remains subdominant within the single-field attractor, the notion of particle number for each species is well-defined in that limit, and we may relate $\rho_k^{(\phi)}$ and $\rho_k^{(\chi)}$ to the corresponding number densities of produced particles.

To calculate the number density of created particles and relate those expressions to adiabatic parameters, we generalize the familiar result from studies of single-field models with minimal couplings. (See also [52, 99–101].) Within the single-field attractor, the coupled equations of motion in Eq. (70) reduce to

$$\begin{aligned} v_k'' + \Omega_{(\phi)}^2(k, \eta) v_k &\simeq 0, \\ z_k'' + \Omega_{(\chi)}^2(k, \eta) z_k &\simeq 0. \end{aligned} \quad (79)$$

We are interested in how efficiently the background fields φ^I transfer energy to the fluctuations after the end of inflation, so we quantize the fluctuations with respect to the adiabatic vacuum $|0(t_{\text{end}})\rangle$, that is, the state that instantaneously minimizes the system's energy at t_{end} [21, 30, 32].

We then posit solutions to Eq. (79) of the form

$$\begin{aligned} v_k(\eta) &= \frac{1}{\sqrt{2W_{(\phi)}(k, \eta)}} \exp \left[-i \int^\eta d\eta' W_{(\phi)}(k, \eta') \right], \\ z_k(\eta) &= \frac{1}{\sqrt{2W_{(\chi)}(k, \eta)}} \exp \left[-i \int^\eta d\eta' W_{(\chi)}(k, \eta') \right], \end{aligned} \quad (80)$$

in terms of the (as yet unspecified) real-valued functions $W_{(I)}(k, \eta)$. The choice of adiabatic vacuum corresponds to the boundary conditions $W_{(\phi)}(k, \eta_{\text{end}}) = \Omega_{(\phi)}(k, \eta_{\text{end}})$ and $W_{(\chi)}(k, \eta_{\text{end}}) = \Omega_{(\phi)}(k, \eta_{\text{end}})$. Given the ansatz in Eq. (80), the expressions in Eq. (75) for the energy density per mode take the form

$$\rho_k^{(\phi)} = \frac{1}{2} \left[W_{(\phi)} + \frac{W_{(\phi)}''}{4W_{(\phi)}^2} - \frac{W_{(\phi)}'^2}{4W_{(\phi)}^3} \right] + \mathcal{O}(\chi^2), \quad (81)$$

and likewise for $\rho_k^{(\chi)}$ in terms of $W_{(\chi)}$ and its derivatives.

Within the single-field attractor, when $\rho_k^{(\text{int})} \sim 0$ and $\rho_k^{(\phi)}$ and $\rho_k^{(\chi)}$ assume the simple forms in Eq. (78), the number densities in Eq. (76) likewise simplify. We may also use Eq. (79) to relate $W_{(\phi)}(k, \eta)$ to $\Omega_{(\phi)}(k, \eta)$, which yields

$$W_{(\phi)}^2 = \Omega_{(\phi)}^2 - \frac{1}{2} \left[\frac{W_{(\phi)}''}{W_{(\phi)}} - \frac{3}{2} \frac{W_{(\phi)}'}{W_{(\phi)}^2} \right]. \quad (82)$$

Away from resonance bands we expect the modes to evolve adiabatically, for which $W_{(\phi)}(k, \eta) \rightarrow \Omega_{(\phi)}(k, \eta) + \mathcal{O}(\mathcal{A}_{(\phi)}^2)$, where

$$\mathcal{A}_{(\phi)}(k, \eta) \equiv \frac{\Omega_{(\phi)}'(k, \eta)}{\Omega_{(\phi)}^2(k, \eta)}. \quad (83)$$

As in [30], we may then solve Eq. (82) iteratively, in increasing powers of $\mathcal{A}_{(\phi)}$. Combining Eqs. (81) - (83), we find

$$n_k^{(\phi)} = \frac{1}{16} \mathcal{A}_{(\phi)}^2 + \mathcal{O}(\chi^2) + \mathcal{O}(\mathcal{A}_{(\phi)}^3), \quad (84)$$

with a comparable expression for $n_k^{(\chi)}$. Much as in familiar cases with minimally coupled fields [21, 52, 99, 100], regions of parameter space in which $\mathcal{A}_{(I)}(k, \eta) \gg 1$ correspond to strong departures from adiabatic evolution, and hence to bursts of particle production.

B. Resonant Amplification within the Attractor

The behavior of the adiabatic parameters, $\mathcal{A}_{(I)}(k, \eta)$, depends upon the effective frequencies, $\Omega_{(I)}(k, \eta)$, which in turn depend upon the effective masses, $m_{\text{eff}, I}^2$, defined in Eq. (72). After the end of inflation, as $\varphi^I(t)$ oscillates, one or more of the $m_{\text{eff}, I}^2$ will oscillate as well, which can drive resonant amplification of the coupled fluctuations, \hat{Q}^I . In the limit $k \ll aH$, we expect $|\mathcal{A}_{(I)}| \gg 1$ whenever $m_{\text{eff}, I}$ passes through zero. Given the form of Eq. (72), we may distinguish four separate contributions to $m_{\text{eff}, I}$:

$$m_{\text{eff}, \phi}^2 = m_{1, \phi}^2 + m_{2, \phi}^2 + m_{3, \phi}^2 + m_{4, \phi}^2, \quad (85)$$

where

$$\begin{aligned}
m_{1,\phi}^2 &\equiv \mathcal{G}^{\phi K} (\mathcal{D}_\phi \mathcal{D}_K V), \\
m_{2,\phi}^2 &\equiv -\mathcal{R}_{LM\phi}^\phi \dot{\phi}^L \dot{\phi}^M, \\
m_{3,\phi}^2 &\equiv -\frac{1}{M_{\text{pl}}^2 a^3} \delta_I^\phi \delta_\phi^J \mathcal{D}_t \left(\frac{a^3}{H} \dot{\phi}^I \dot{\phi}_J \right), \\
m_{4,\phi}^2 &\equiv -\frac{1}{6} R,
\end{aligned} \tag{86}$$

with comparable expressions for the contributions to $m_{\text{eff},\chi}^2$. Note that $m_{1,I}^2$ arises from the gradient of the potential; $m_{2,I}^2$ from the nontrivial field-space manifold; $m_{3,I}^2$ from the coupled metric perturbations; and $m_{4,I}^2$ from changes in the background spacetime.

We first note that

$$m_{4,I}^2 = -\frac{1}{6} R = -\left(\dot{H} + 2H^2 \right) = (\epsilon - 2)H^2. \tag{87}$$

We observed in Section III B that in general $\epsilon = 3\dot{\sigma}^2/(\dot{\sigma}^2 + 2V)$, so $0 \leq \epsilon \leq 3$, and hence $m_{4,I}^2/H^2 = \mathcal{O}(1)$ independent of the couplings and of the motion of the background fields φ^I . Within the single-field attractor (with $\chi \sim \dot{\chi} \sim 0$), many of the other terms in Eq. (86) also become negligible. In particular,

$$\begin{aligned}
\mathcal{G}_{\phi\chi} &\sim \mathcal{G}^{\phi\chi} \sim \mathcal{O}(\chi) \sim 0, \\
\Gamma_{\phi\chi}^\phi &\sim \Gamma_{\phi\phi}^\chi \sim \Gamma_{\chi\chi}^\chi \sim \mathcal{O}(\chi) \sim 0, \\
V_{,\chi} &\sim V_{,\phi\chi} \sim \mathcal{O}(\chi) \sim 0.
\end{aligned} \tag{88}$$

Upon using the expressions for \mathcal{G}_{IJ} , Γ_{JK}^I , and \mathcal{R}_{ILMJ} in Appendix A, we then find

$$\begin{aligned}
m_{1,\phi}^2 &= \mathcal{G}^{\phi\phi} \left[V_{,\phi\phi} - \Gamma_{\phi\phi}^\phi V_{,\phi} \right] + \mathcal{O}(\chi^2), \\
m_{2,\phi}^2 &= \mathcal{O}(\chi\dot{\chi}) \sim 0, \\
m_{3,\phi}^2 &= -\frac{\mathcal{G}_{\phi\phi}}{M_{\text{pl}}^2} \left[(3 + \epsilon)\dot{\phi}^2 + \frac{2}{H}\dot{\phi}\ddot{\phi} \right] + \mathcal{O}(\chi\dot{\chi}), \\
m_{1,\chi}^2 &= \mathcal{G}^{\chi\chi} \left[V_{,\chi\chi} - \Gamma_{\chi\chi}^\phi V_{,\phi} \right] + \mathcal{O}(\chi^2), \\
m_{2,\chi}^2 &= \frac{1}{2} \mathcal{R}_{\phi\phi} \dot{\phi}^2 + \mathcal{O}(\chi\dot{\chi}), \\
m_{3,\chi}^2 &= \mathcal{O}(\chi\dot{\chi}) \sim 0.
\end{aligned} \tag{89}$$

The \mathcal{R} in $m_{2,\chi}^2$ is the Ricci curvature scalar of the field-space manifold, an explicit expression for which may be found in Eq. (109) in Appendix A. Numerical calculation confirms that the contributions to $m_{\text{eff},I}^2$ that arise from a nonrigid spacetime — that is, $m_{3,I}^2$ and $m_{4,I}^2$ — remain

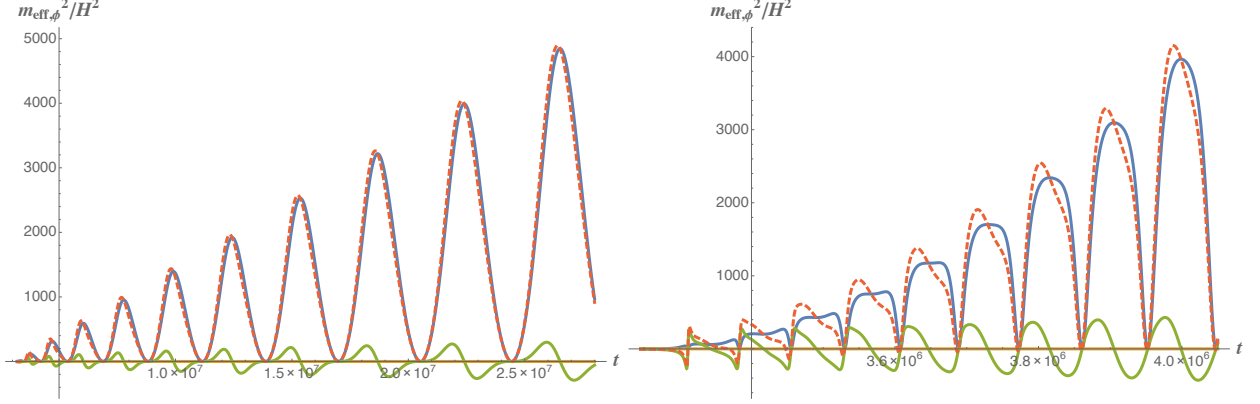


FIG. 9: The contributions $m_{1,\phi}^2/H^2$ (blue), $m_{2,\phi}^2/H^2$ (gold), and $m_{3,\phi}^2/H^2$ (green) compared to $m_{\text{eff},\phi}^2/H^2$ (red dashed) for $\xi_\chi/\xi_\phi = 0.8$, $\lambda_\chi/\lambda_\phi = 1.25$, and $g/\lambda_\phi = 1$, with $\xi_\phi = 10^{-1}$, $\lambda_\phi = 10^{-10}$ (left) and $\xi_\phi = 10$, $\lambda_\phi = 10^{-6}$ (right). Recall that $m_{1,\phi}^2$ arises from the gradient of the potential, $m_{2,\phi}^2$ from the nontrivial field-space manifold, and $m_{3,\phi}^2$ from the coupled metric perturbations. Note that for both large and small ξ_I , $m_{2,\phi}^2 \sim 0$, and $m_{3,\phi}^2 \ll m_{\text{eff},\phi}^2$ after the first few oscillations, so that for both $\xi_I \leq 1$ and $\xi_I \gg 1$, $m_{\text{eff},\phi}^2$ is dominated by $m_{1,\phi}^2$. In all cases, $m_{\text{eff},\phi}^2/H^2$ grows over time because $H(t)$ falls after the end of inflation.

subdominant in both the adiabatic and isocurvature directions, for both $\xi_I \leq 1$ and $\xi_I \gg 1$. (In the limit $\xi_I \gg 1$, $m_{3,\phi}^2$ can be comparable to $m_{\text{eff},\phi}^2$ for the first few oscillations of the background fields, but quickly becomes subdominant.) In the limit $m_{3,I}^2, m_{4,I}^2 \ll m_{\text{eff},I}^2$, the full structure of the resonance bands may be analyzed using Floquet theory [51].

A significant difference arises among the other two contributions to $m_{\text{eff},I}^2$, from the gradient of the potential ($m_{1,I}^2$) and from the nontrivial field-space manifold ($m_{2,I}^2$). Along the adiabatic direction, the contribution to $m_{\text{eff},\phi}^2$ from $m_{2,\phi}^2$ always remains negligible, independent of the magnitude of ξ_I , leaving $m_{\text{eff},\phi}^2 \sim m_{1,\phi}^2$, which repeatedly oscillates through zero as $\phi(t)$ oscillates. On the other hand, along the isocurvature direction, $m_{2,\chi}^2 \propto \dot{\phi}^2$ may become comparable in magnitude, but opposite in phase, to $m_{1,\chi}^2 \propto \phi^2$ in the limit $\xi_I \gg 1$. Hence in the large- ξ_I limit, although the effective mass in the adiabatic direction, $m_{\text{eff},\phi}^2$, repeatedly oscillates through zero, the effective mass in the isocurvature direction, $m_{\text{eff},\chi}^2$, does not. See Figs. 9 and 10.

We may make sense of the behavior of $m_{1,\chi}^2$ and $m_{2,\chi}^2$ analytically. In the limit $\xi_I \ll 1$, we have

$$m_{1,\chi}^2 = \frac{gM_{\text{pl}}^2}{\xi_\phi} \delta^2 \left[1 - \delta^2 \left(1 + \frac{\lambda_\phi}{g} (2 - \varepsilon) \right) \right] + \mathcal{O}(\xi_I^2), \quad (90)$$

where δ^2 is defined in Eq. (24) and the eccentricity ε is defined in Eq. (27). In the same limit, we have

$$m_{2,\chi}^2 = \left(\frac{\dot{\phi}^2}{M_{\text{pl}}^4} \right) [\xi_\phi + \xi_\chi] + \mathcal{O}(\xi_I^2). \quad (91)$$

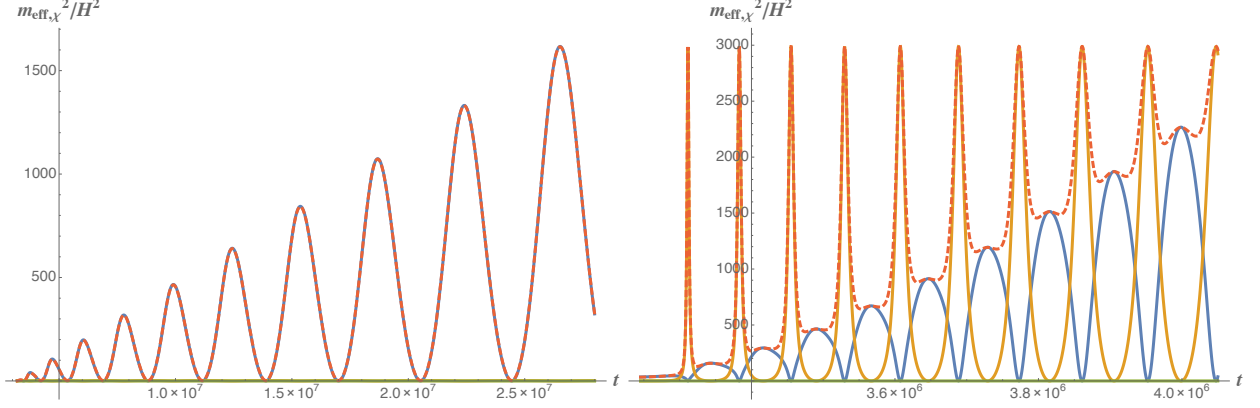


FIG. 10: The contributions $m_{1,\chi}^2/H^2$ (blue), $m_{2,\chi}^2/H^2$ (gold), and $m_{3,\chi}^2/H^2$ (green) compared to $m_{\text{eff},\chi}^2/H^2$ (red dashed) for $\xi_\chi/\xi_\phi = 0.8$, $\lambda_\chi/\lambda_\phi = 1.25$, and $g/\lambda_\phi = 1$, with $\xi_\phi = 10^{-1}$, $\lambda_\phi = 10^{-10}$ (left) and $\xi_\phi = 10$, $\lambda_\phi = 10^{-6}$ (right). Note that $m_{3,\chi}^2 \sim 0$ for both large and small ξ_I , and that for $\xi_I \ll 1$, $m_{2,\chi}^2 \ll m_{1,\chi}^2$, so that $m_{\text{eff},\chi}^2$ is dominated by $m_{1,\chi}^2$. However, for $\xi_I \gg 1$, both $m_{1,\chi}^2$ and $m_{2,\chi}^2$ remain comparable in magnitude and opposite in phase, so that $m_{\text{eff},\chi}^2$ never passes through zero.

For an order-of-magnitude estimate, we may approximate $\dot{\phi}^2 \sim \omega^2 \phi^2$ and use our results from Section III C. In the limit $\xi_I \ll 1$, we have $\omega = 2\pi/T \rightarrow (2\pi/3.9)\sqrt{\lambda_\phi} M_{\text{pl}}$ and hence

$$\frac{m_{2,\chi}^2}{m_{1,\chi}^2} \sim \frac{\lambda_\phi}{g} (\xi_\phi + \xi_\chi) + \mathcal{O}(\xi_I^2). \quad (92)$$

For $\xi_I \ll 1$, we therefore find a clear separation of scales, $m_{2,\chi}^2 \ll m_{1,\chi}^2$. In that limit, $m_{\text{eff},\chi}^2 \simeq m_{1,\chi}^2$ and $m_{\text{eff},\chi}^2$ passes near zero as the background field $\phi(t)$ oscillates, as shown in Fig. 10a. In the opposite limit, $\xi_I \gg 1$, however, we find

$$m_{1,\chi}^2 = -\frac{\Lambda_\phi}{\xi_\phi^2} M_{\text{pl}}^2 \left(\frac{\delta^2}{1 + \delta^2} \right) + \mathcal{O}(\xi_I^{-2}), \quad (93)$$

where Λ_ϕ is defined in Eq. (27). In the limit $\xi_I \gg 1$, the parameter $\delta^2 \sim \mathcal{O}(1)$ at the end of inflation. Upon using Eq. (109), we find

$$m_{2,\chi}^2 = \frac{6\xi_\phi \xi_\chi}{M_{\text{pl}}^2} \dot{\phi}^2 + \mathcal{O}(\xi_I). \quad (94)$$

Again making use of our results in Section III C to replace $\dot{\phi}^2 \sim \omega^2 \phi^2$, now in the limit $\xi_I \gg 1$, we have $\omega = 2\pi/T \rightarrow (2\pi/14.8)\sqrt{\lambda_\phi} M_{\text{pl}}/\xi_\phi$, which yields

$$\frac{m_{2,\chi}^2}{m_{1,\chi}^2} \sim \frac{\lambda_\phi \xi_\chi}{|\Lambda_\phi|} \sim \mathcal{O}(1). \quad (95)$$

Therefore we do indeed expect $m_{1,\chi}^2$ and $m_{2,\chi}^2$ to remain comparable in magnitude but opposite in phase in the limit $\xi_I \gg 1$. In that case, $m_{\text{eff},\chi}^2$ never passes through zero, as shown in Fig. 10b.

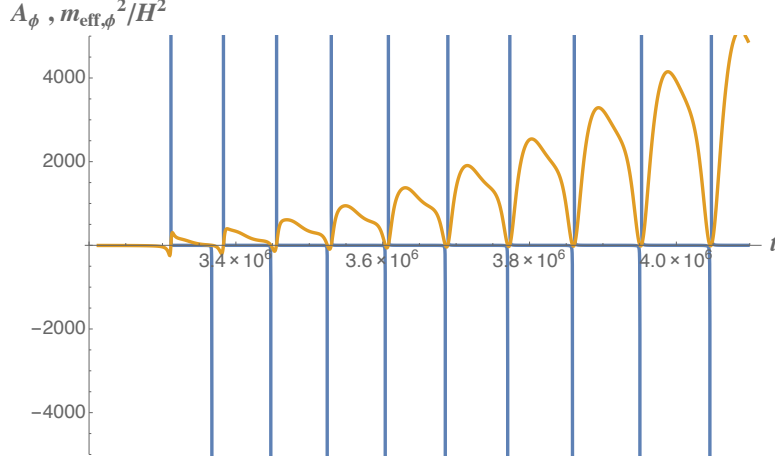


FIG. 11: The adiabatic parameter $\mathcal{A}_{(\phi)}(t)$ (blue) and the effective mass $m_{\text{eff},\phi}^2/H^2$ (gold) for $\xi_\chi/\xi_\phi = 0.8$, $\lambda_\chi/\lambda_\phi = 1.25$, $g/\lambda_\phi = 1$, and $k \ll aH$, with $\xi_\phi = 10$, $\lambda_\phi = 10^{-6}$. Note that $|\mathcal{A}_{(\phi)}|$ spikes each time $m_{\text{eff},\phi}^2$ passes through zero.

The different behavior of $m_{\text{eff},\phi}^2$ and $m_{\text{eff},\chi}^2$ in the limit $\xi_I \gg 1$ leads to different behavior for the adiabatic parameters, $\mathcal{A}_{(\phi)}$ and $\mathcal{A}_{(\chi)}$. We may rewrite Eq. (83) in terms of cosmic time rather than conformal time,

$$\mathcal{A}_{(\phi)} = \frac{H^{-3} \partial_t m_{\text{eff},\phi}^2 + 2(m_{\text{eff},\phi}/H)^2}{2[\ell^2 + (m_{\text{eff},\phi}/H)^2]^{3/2}}, \quad (96)$$

where $\ell \equiv k_{\text{phys}}/H = k/(aH)$. In the limit $\ell \ll 1$, we find

$$\mathcal{A}_{(\phi)} = \frac{\partial_t m_{\text{eff},\phi}^2}{2m_{\text{eff},\phi}^3} + \frac{H}{m_{\text{eff},\phi}} + \mathcal{O}(\ell^2). \quad (97)$$

As expected, $|\mathcal{A}_{(\phi)}| \gg 1$ whenever $m_{\text{eff},\phi}^2$ passes through zero, as shown in Fig. 11. On the other hand, although $\partial_t m_{\text{eff},\chi}^2$ repeatedly spikes to be large in the limit $\xi_I \gg 1$, the ratio $\partial_t m_{\text{eff},\chi}^2/m_{\text{eff},\chi}^3$ remains $\mathcal{O}(1)$, and hence so does $|\mathcal{A}_{(\chi)}|$, as shown in Fig. 12. As we tune ξ_I to smaller values, the quantities $m_{1,\chi}^2$ and $m_{2,\chi}^2$ separate in scale, $m_{\text{eff},\chi}^2$ passes closer to zero during $\phi(t)$'s oscillations, and the adiabatic parameter $\mathcal{A}_{(\chi)}$, like $\mathcal{A}_{(\phi)}$, repeatedly spikes to large values. See Fig. 13. Given the relations derived above between $\mathcal{A}_{(I)}$ and $n_k^{(I)}$, the spikes in $\mathcal{A}_{(I)}$ correspond to rapid bursts of particle production and thus the transfer of energy from the background fields φ^I to the coupled fluctuations.

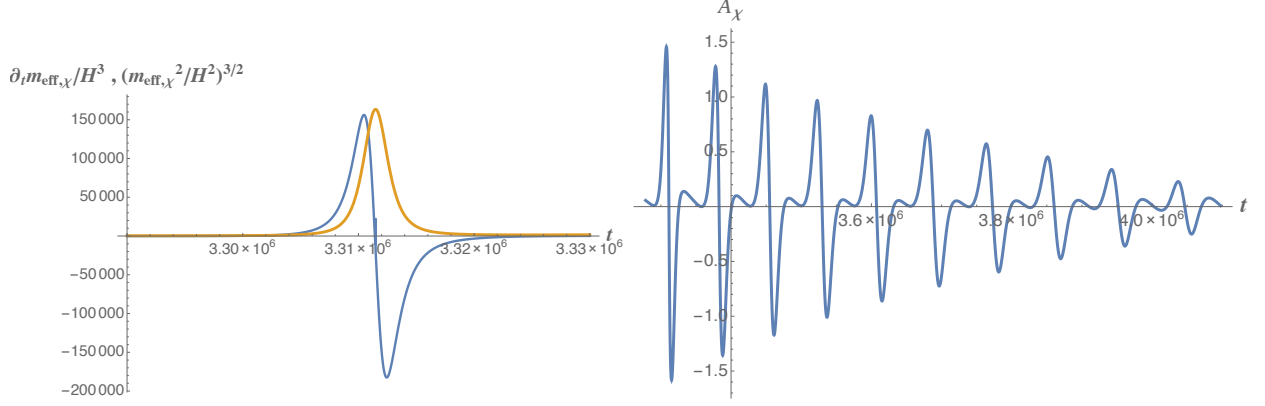


FIG. 12: (Left) The quantities $H^{-3} \partial_t m_{\text{eff},\chi}^2$ (blue) and $(m_{\text{eff},\chi}^2/H^2)^{3/2}$ (gold) for $\xi_\chi/\xi_\phi = 0.8$, $\lambda_\chi/\lambda_\phi = 1.25$, $g/\lambda = 1$, with $\xi_\phi = 10$, $\lambda_\phi = 10^{-6}$. Even though $\partial_t m_{\text{eff},\chi}^2$ spikes to be very large, the value of $m_{\text{eff},\chi}^3$ remains comparable and hence $\mathcal{A}_{(\chi)} \sim \mathcal{O}(1)$. (Right) The adiabatic parameter $\mathcal{A}_{(\chi)}$ for the same couplings and $k \ll aH$.

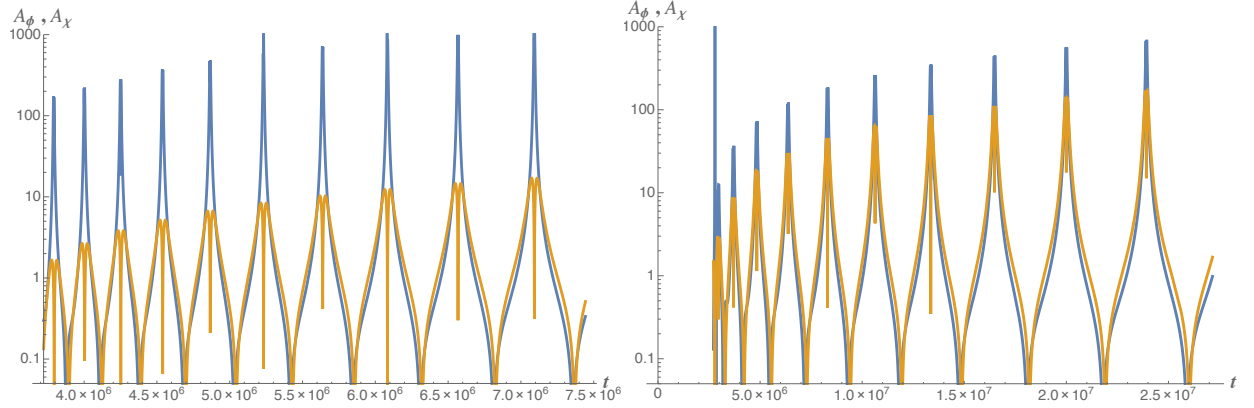


FIG. 13: The adiabatic parameters $\mathcal{A}_{(\phi)}$ (blue) and $\mathcal{A}_{(\chi)}$ (gold) for $k \ll aH$ with $\xi_\chi/\xi_\phi = 0.8$, $\lambda_\chi/\lambda_\phi = 1.25$, $g/\lambda_\phi = 1$, and $\xi_\phi = 1$, $\lambda_\phi = 10^{-8}$ (left) and $\xi_\phi = 10^{-1}$, $\lambda_\phi = 10^{-10}$ (right).

C. Rotating the Field-Space Coordinates

Now consider what happens when we change the couplings so that the single-field attractor lies along some distinct direction in field space. For example, we may select the couplings

$$\frac{\lambda_\chi}{\lambda_\phi} = 1.25, \quad \frac{g}{\lambda_\phi} = -1/2, \quad \frac{\xi_\chi}{\xi_\phi} = 0.8. \quad (98)$$

For minimally coupled models, $g < 0$ leads to an explosive “negative coupling instability” for long-wavelength modes [102, 103]. In the presence of nonminimal couplings, however, at least for $|g| \sim \mathcal{O}(\lambda_\phi)$, the effect of the negative coupling is to rotate the orientation of the valley of the potential away from the direction $\chi = 0$. See Fig. 14. With the fields’ motion “misaligned” with respect to the original axes of our field-space coordinate system, we find suppression of the

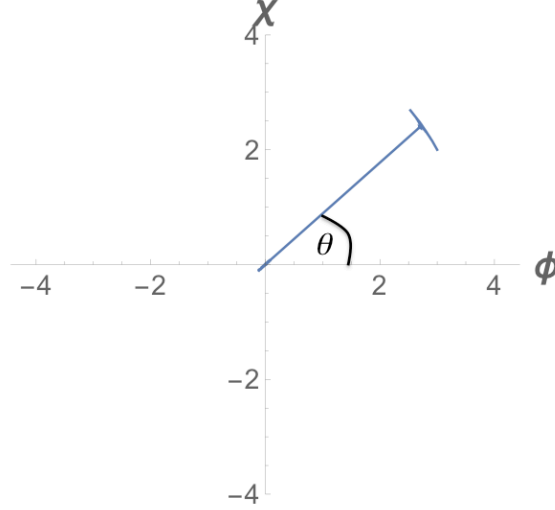


FIG. 14: For some choices of the coupling constants, the background fields evolve along a single-field trajectory at some angle θ that does not coincide with either the ϕ or χ axes. Shown here is the case for $\xi_\chi/\xi_\phi = 0.8$, $\lambda_\chi/\lambda_\phi = 1.25$, $g/\lambda_\phi = -1/2$, with $\xi_\phi = 10$, $\lambda_\phi = 10^{-6}$. The angle, $\theta = \arctan(\chi/\phi)$, is independent of time during as well as after inflation.

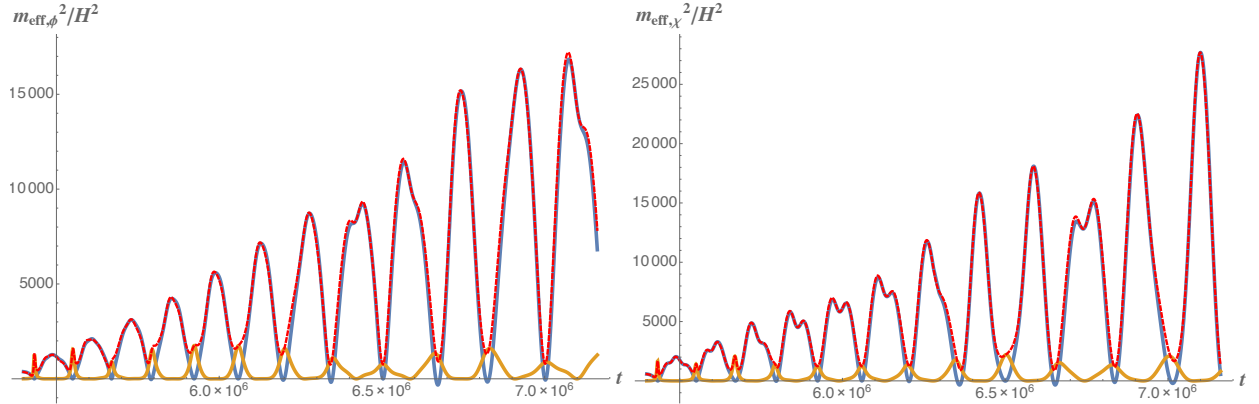


FIG. 15: (*Left*) The terms $m_{1,\phi}^2$ (blue) and $m_{2,\phi}^2$ (gold) compared to $m_{\text{eff},\phi}^2$ (dashed red) for $\xi_\phi = 10$, $g = -1/2$, and the other couplings as in Eq. (98). When plotted with respect to the original coordinate bases, $m_{\text{eff},\phi}^2$ no longer oscillates through zero. (*Right*) The terms $m_{1,\chi}^2$ (blue) and $m_{2,\chi}^2$ (gold) compared to $m_{\text{eff},\chi}^2$ (dashed red) for $\xi_\phi = 10$, $g = -1/2$, and the other couplings as in Eq. (98).

resonances along *both* of the original axes, since in this case $m_{2,I}^2$ remains comparable in magnitude (but opposite in phase) with $m_{1,I}^2$ for both $m_{\text{eff},\phi}^2$ and $m_{\text{eff},\chi}^2$. See Fig. 15. Therefore both $\mathcal{A}_{(\phi)}$ and $\mathcal{A}_{(\chi)}$ remain $\mathcal{O}(1)$, as shown in Fig. 16.

However, as Fig. 14 makes clear, in this case the fields still evolve within a single-field attractor. We may parameterize the motion by a single angle, $\theta \equiv \arctan(\chi/\phi)$, which does not vary over time (even after t_{end}). That is, when plotted in the original coordinate system, the background

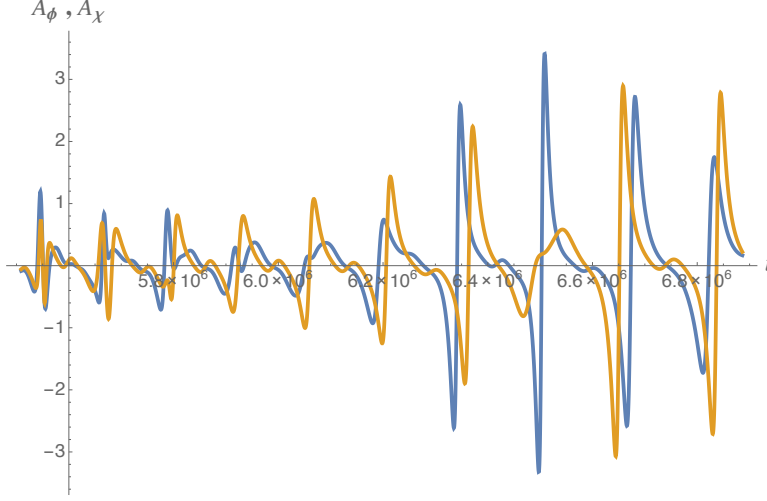


FIG. 16: The adiabatic parameters $\mathcal{A}_{(\phi)}$ and $\mathcal{A}_{(\chi)}$ for $\xi_\phi = 10$, $g = -1/2$, and the other couplings as in Eq. (98). Because $m_{2,I}^2$ remains comparable in magnitude but opposite in phase to $m_{1,I}^2$, neither $\mathcal{A}_{(\phi)}$ nor $\mathcal{A}_{(\chi)}$ grows much larger than 1.

fields' motion obeys

$$\phi(t) = r(t) \cos \theta, \quad \chi(t) = r(t) \sin \theta. \quad (99)$$

We may then perform a rotation of our coordinates in field space so that the single-field attractor lies along the $\bar{\chi}$ direction, with all motion of the background fields along the $\bar{\phi}$ axis. (In this subsection we denote the rotated coordinate system with an overbar rather than a prime, to avoid confusion with derivatives, $d/d\eta$.) Hence we may write

$$\begin{aligned} \bar{\phi} &= \phi \cos \theta + \chi \sin \theta, \\ \bar{\chi} &= \chi \cos \theta - \phi \sin \theta. \end{aligned} \quad (100)$$

Components of the tensor $[\omega_k^2]^I_J$ transform in the usual way under this coordinate transformation:

$$[\bar{\omega}_k^2]^I_J = \left(\frac{\partial \bar{\varphi}^I}{\partial \varphi^K} \right) \left(\frac{\partial \varphi^L}{\partial \bar{\varphi}^J} \right) [\omega_k^2]^K_L. \quad (101)$$

In particular, we find

$$\begin{aligned} [\bar{\omega}_k^2]^\phi_\phi &= \cos^2 \theta [\omega_k^2]^\phi_\phi + \sin \theta \cos \theta \left([\omega_k^2]^\chi_\phi + [\omega_k^2]^\phi_\chi \right) + \sin^2 \theta [\omega_k^2]^\chi_\chi, \\ [\bar{\omega}_k^2]^\chi_\chi &= \cos^2 \theta [\omega_k^2]^\chi_\chi - \sin \theta \cos \theta \left([\omega_k^2]^\phi_\chi + [\omega_k^2]^\chi_\phi \right) + \sin^2 \theta [\omega_k^2]^\phi_\phi. \end{aligned} \quad (102)$$

When plotted with respect to the rotated coordinate system, we recover the type of behavior we had found in Section IV B for a single-field attractor along the direction $\chi = 0$. Fig. 17 shows the dominant contributions to $\bar{m}_{\text{eff},\phi}^2$, revealing that in the rotated coordinate system, the

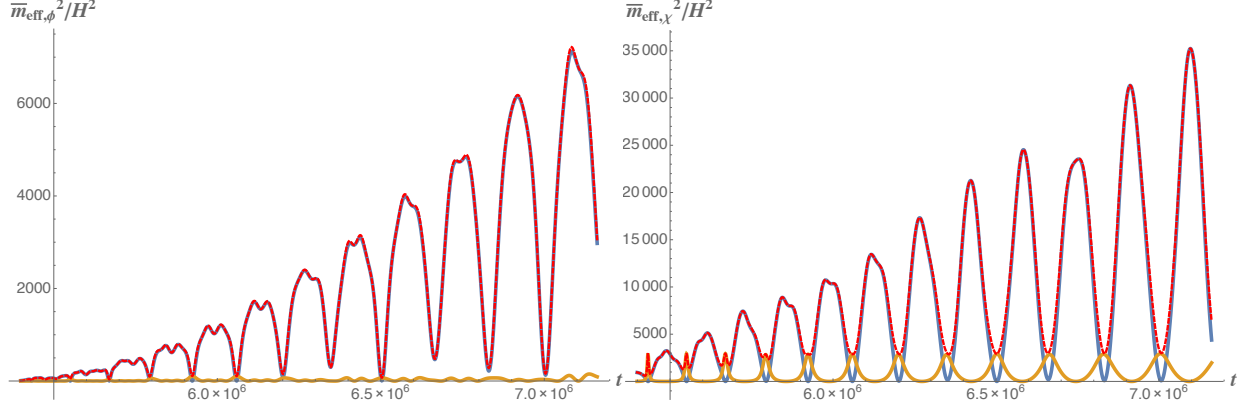


FIG. 17: (*Left*) The contributions $\bar{m}_{1,\phi}^2$ (blue) and $\bar{m}_{2,\phi}^2$ (gold) to $\bar{m}_{\text{eff},\phi}^2$ (red dashed), upon making the rotation in field space, for $\xi_\phi = 10$, $g = -1/2$, and the other couplings as in Eq. (98). Unlike in Fig. 15, here we find the contribution from the field-space manifold, $\bar{m}_{2,\phi}^2$, negligible, and hence $\bar{m}_{\text{eff},\phi}^2 \sim \bar{m}_{1,\phi}^2$ oscillates through zero. (*Right*) The contributions $\bar{m}_{1,\chi}^2$ (blue) and $\bar{m}_{2,\chi}^2$ (gold) to $\bar{m}_{\text{eff},\chi}^2$ (red dashed), upon making the rotation in field space, for $\xi_\phi = 10$, $g = -1/2$, and the other couplings as in Eq. (98).

Just as in the case when the single-field attractor lay along the direction $\chi = 0$, in this case we find $\bar{m}_{1,\chi}^2 \sim \bar{m}_{2,\chi}^2$ but out of phase with each other, so that $\bar{m}_{\text{eff},\chi}^2$ never oscillates through zero.

contributions from the field-space manifold become negligible, just as they do for $m_{\text{eff},\phi}^2$ when the single-field attractor lies along the $\chi = 0$ direction (as in Fig. 9). On the other hand, in the rotated coordinate basis, $\bar{m}_{2,\chi}^2$ remains comparable in magnitude to $\bar{m}_{1,\chi}^2$ but with opposite phase, so that $\bar{m}_{\text{eff},\chi}^2$ never oscillates through zero (akin to the behavior in Fig. 10). Moreover, if we compute

$$\bar{\mathcal{A}}_{(\phi)}(\eta) = \frac{\partial_t \bar{m}_{\text{eff},\phi}^2}{2 \left(\bar{m}_{\text{eff},\phi}^2 \right)^{3/2}} + \frac{H}{\bar{m}_{\text{eff},\phi}} \quad (103)$$

and likewise for $\bar{\mathcal{A}}_{(\chi)}$, we find behavior akin to the original analysis for the $\chi = 0$ attractor, as shown in Fig. 18. Thus we surmise that within *any* single-field attractor, in the limit of $\xi_I \gg 1$, we find suppression of the resonances for the isocurvature direction and amplification of the fluctuations along the adiabatic direction. This general result holds even though the models we consider do not obey an $O(N)$ symmetry.

V. CONCLUSIONS

Realistic models of high-energy physics typically include multiple scalar fields, each with its own nonminimal coupling. In this paper we have demonstrated that preheating after inflation in such models introduces unique features that are distinct from other well-studied models of preheating.

In particular, nonminimally coupled fields yield a conformally stretched effective potential in the Einstein frame. In previous work we had highlighted a generic feature that arises from such

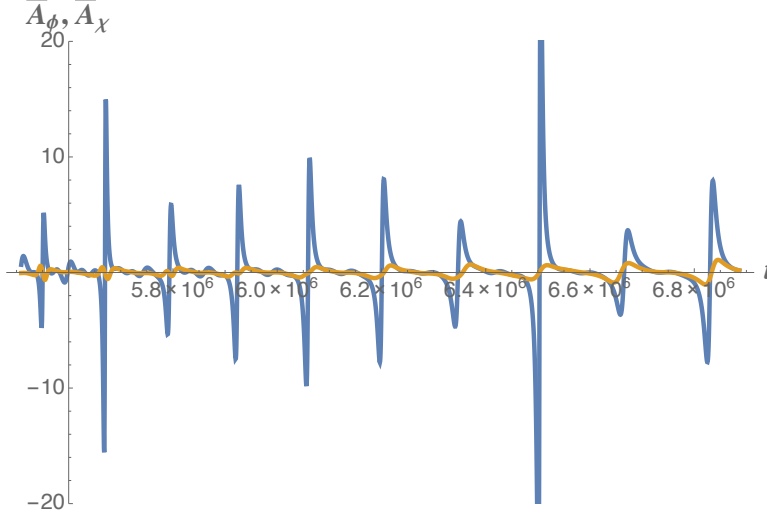


FIG. 18: The adiabatic parameters $\bar{A}_{(\phi)}$ (blue) and $\bar{A}_{(\chi)}$ (gold) with $\xi_\phi = 10$, $g = -1/2$, and the other couplings as in Eq. (98), upon performing the rotation in field space. Here we recover behavior akin to the original example, when the single-field attractor lay along the direction $\chi = 0$: fluctuations along the adiabatic direction become strongly amplified, but those in the isocurvature direction do not.

conformal stretching, namely, the existence of strong single-field attractor behavior across a wide range of couplings and initial conditions [33–36]. Here we have found two main effects related to the conformal stretching and attractor behavior: the effectively single-field evolution of the background fields $\varphi^I(t)$ persists during the oscillatory phase — thereby avoiding the “de-phasing” that is typical of preheating with minimally coupled scalar fields — and the conformal stretching of the potential alters the time-evolution of $\varphi^I(t)$ as the background field(s) oscillate around the global minimum of the potential.

The persistence of the single-field attractor during the preheating phase leads to efficient transfer of energy from the background fields to coupled fluctuations. The balance of the transfer to fluctuations in the adiabatic versus isocurvature directions shifts as the nonminimal coupling constants grow larger. In the limit $\xi_I \gg 1$, we find suppression of growth in the long-wavelength limit for isocurvature modes, but efficient amplification of adiabatic modes. This effect arises entirely from the nontrivial field-space manifold, and has no analogue in models with minimally coupled fields.

In [51] we utilize Floquet analysis to more thoroughly explore the resonance structure in such models as functions of wavenumber, k , as well as coupling constants, ξ_I , λ_I , and g . Other effects also deserve further attention. In particular, the conformal stretching of the potential in the Einstein frame strongly suggests that these models could produce metastable oscillons after inflation [104, 105]. The formation of such long-lived, topologically metastable objects could become important

after the earliest stages of preheating, impacting the rate at which the system ultimately reaches thermal equilibrium. Such effects could therefore affect the final reheat temperature and the expansion history of the universe after inflation. These possibilities remain the subject of further research.

APPENDIX A: FIELD-SPACE METRIC AND RELATED QUANTITIES

Given $f(\phi^I)$ in Eq. (19) for a two-field model, the field-space metric in the Einstein frame, Eq. (5), takes the form

$$\begin{aligned}\mathcal{G}_{\phi\phi} &= \left(\frac{M_{\text{pl}}^2}{2f}\right) \left[1 + \frac{3\xi_\phi^2\phi^2}{f}\right], \\ \mathcal{G}_{\phi\chi} = \mathcal{G}_{\chi\phi} &= \left(\frac{M_{\text{pl}}^2}{2f}\right) \left[\frac{3\xi_\phi\xi_\chi\phi\chi}{f}\right], \\ \mathcal{G}_{\chi\chi} &= \left(\frac{M_{\text{pl}}^2}{2f}\right) \left[1 + \frac{3\xi_\chi^2\chi^2}{f}\right].\end{aligned}\tag{104}$$

The components of the inverse metric are

$$\begin{aligned}\mathcal{G}^{\phi\phi} &= \left(\frac{2f}{M_{\text{pl}}^2}\right) \left[\frac{2f + 6\xi_\chi^2\chi^2}{C}\right], \\ \mathcal{G}^{\phi\chi} = \mathcal{G}^{\chi\phi} &= -\left(\frac{2f}{M_{\text{pl}}^2}\right) \left[\frac{6\xi_\phi\xi_\chi\phi\chi}{C}\right], \\ \mathcal{G}^{\chi\chi} &= \left(\frac{2f}{M_{\text{pl}}^2}\right) \left[\frac{2f + 6\xi_\phi^2\phi^2}{C}\right],\end{aligned}\tag{105}$$

where $C(\phi^I)$ is defined as

$$\begin{aligned}C(\phi, \chi) &\equiv M_{\text{pl}}^2 + \xi_\phi(1 + 6\xi_\phi)\phi^2 + \xi_\chi(1 + 6\xi_\chi)\chi^2 \\ &= 2f + 6\xi_\phi^2\phi^2 + 6\xi_\chi^2\chi^2.\end{aligned}\tag{106}$$

The Christoffel symbols for our field space take the form

$$\begin{aligned}\Gamma_{\phi\phi}^\phi &= \frac{\xi_\phi(1 + 6\xi_\phi)\phi}{C} - \frac{\xi_\phi\phi}{f}, \\ \Gamma_{\chi\phi}^\phi = \Gamma_{\phi\chi}^\phi &= -\frac{\xi_\chi\chi}{2f}, \\ \Gamma_{\chi\chi}^\phi &= \frac{\xi_\phi(1 + 6\xi_\chi)\phi}{C}, \\ \Gamma_{\phi\phi}^\chi &= \frac{\xi_\chi(1 + 6\xi_\phi)\chi}{C}, \\ \Gamma_{\phi\chi}^\chi = \Gamma_{\chi\phi}^\chi &= -\frac{\xi_\phi\phi}{2f}, \\ \Gamma_{\chi\chi}^\chi &= \frac{\xi_\chi(1 + 6\xi_\chi)\chi}{C} - \frac{\xi_\chi\chi}{f}\end{aligned}\tag{107}$$

For two-dimensional manifolds we may always write the Riemann tensor in the form

$$\mathcal{R}_{ABCD} = \frac{1}{2}\mathcal{R}(\phi^I) [\mathcal{G}_{AC}\mathcal{G}_{BD} - \mathcal{G}_{AD}\mathcal{G}_{BC}], \quad (108)$$

where $\mathcal{R}(\phi^I)$ is the Ricci scalar. Given the field-space metric of Eq. (104), we find

$$\mathcal{R}(\phi^I) = \frac{1}{3M_{\text{pl}}^2 C^2} [(1 + 6\xi_\phi)(1 + 6\xi_\chi)(4f^2) - C^2]. \quad (109)$$

For the two-field model, we may also solve explicitly for the vielbeins, e_b^I , of Eq. (63). Defining

$$\begin{aligned} A &\equiv C - 6\xi_\phi^2 \phi^2, \\ B &\equiv C - 6\xi_\chi^2 \chi^2, \\ E &\equiv C - 3\xi_\phi^2 \phi^2 - 3\xi_\chi^2 \chi^2, \\ F &\equiv \frac{\sqrt{2fC} \sqrt{E - 2fC}}{3\sqrt{2} M_{\text{pl}} (\xi_\chi^2 \chi^2 + \xi_\phi^2 \phi^2) C}, \end{aligned} \quad (110)$$

then we may satisfy Eq. (63) with

$$\begin{aligned} e_1^\phi &= F \left(A + \sqrt{2fC} \right), \\ e_1^\chi &= -12F\xi_\phi\xi_\phi\phi\chi, \\ e_2^\phi &= e_1^\chi, \\ e_2^\chi &= F \left(B + \sqrt{2fC} \right). \end{aligned} \quad (111)$$

We note that within the single-field attractor along the direction $\chi = 0$, $e_2^\phi \sim e_1^\chi \sim 0$, $e_1^\phi e_1^\phi \rightarrow \mathcal{G}^{\phi\phi} + \mathcal{O}(\chi^2)$, and $e_2^\chi e_2^\chi \rightarrow \mathcal{G}^{\chi\chi} + \mathcal{O}(\chi^2)$.

APPENDIX B: PERIOD OF SINGLE-FIELD BACKGROUND OSCILLATIONS

Starting from Eq. (49) and inserting the values of $\mathcal{G}_{\phi\phi}$ and $V(\phi)$ the period becomes

$$T = 4\sqrt{2\xi_\phi} \int_0^\alpha du \frac{\sqrt{1 + 6\xi_\phi u^2}}{(1 + u^2)} \frac{1}{\sqrt{\frac{\alpha^4}{(1 + \alpha^2)^2} - \frac{u^4}{(1 + u^2)^2}}} \quad (112)$$

where we proceeded to a change of variables $u = \sqrt{\xi_\phi}\phi$ and the maximum field amplitude is $\phi_{\text{max}} = \alpha M_{\text{pl}}/\sqrt{\xi_\phi}$. By assuming a maximum field amplitude such that $1 < 6\xi_\phi\alpha^2$ and approximating $1 + 6\xi_\phi u^2 \approx 6\xi_\phi u^2$, the integral can be performed analytically and the resulting Eq. (50) shows the linear scaling of the period with ξ_ϕ . The limit of this approximation is shown in Fig. 19, where it can be seen that the agreement between Eq. (50) and the exact result is excellent in the large- ξ_I limit for α not very small. The region of validity in terms of α increases for larger values of ξ_ϕ , as expected from the condition $\alpha > 1/\sqrt{6\xi_\phi}$ used in the derivation of Eq. (50). Fig. 19 shows the period of oscillation for different values of ξ_I and α .

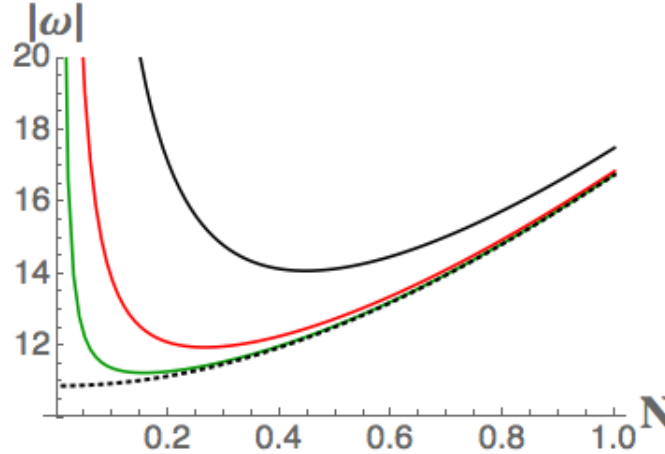


FIG. 19: Period of oscillation rescaled by the nonminimal coupling as a function of $\alpha = \phi_0/M_{\text{pl}}$ for $\xi = 10, 10^2, 10^3$ (from top to bottom). The dashed line shows the approximate analytic result of Eq. (50).

ACKNOWLEDGMENTS

It is a pleasure to thank Mustafa Amin, Bruce Bassett, Jolyon Bloomfield, Peter Fisher, Tom Giblin, Alan Guth, Mark Hertzberg, and Johanna Karouby for helpful discussions. We would like to acknowledge support from the Center for Theoretical Physics at MIT. This work is supported by the U.S. Department of Energy under grant Contract Number de-sc00012567. MPD and AP were also supported in part by MIT's Undergraduate Research Opportunities Program (UROP). EIS gratefully acknowledges support from a Fortner Fellowship at the University of Illinois at Urbana-Champaign. CPW gratefully acknowledges support from the MIT Dr. Martin Luther King, Jr. Visiting Professors and Scholars program and its director Edmund Bertschinger.

-
- [1] A. H. Guth and D. I. Kaiser, “Inflationary cosmology: Exploring the universe from the smallest to the largest scales,” *Science* 307 (2005): 884, arXiv:astro-ph/0502328 [astro-ph].
 - [2] B. A. Bassett, S. Tsujikawa, and D. Wands, “Inflation dynamics and reheating,” *Rev. Mod. Phys.* 78 (2006): 537, arXiv:astro-ph/0507632.
 - [3] D. H. Lyth and A. R. Liddle, *The Primordial Density Perturbation: Cosmology, Inflation, and the Origin of Structure* (New York: Cambridge University Press, 2009).
 - [4] D. Baumann, “TASI Lectures on inflation,” arXiv:0907.5424 [hep-th].
 - [5] J. Martin, C. Ringeval, and V. Vennin, “Encyclopedia inflationaris,” arXiv:1303.3787 [astro-ph.CO].
 - [6] A. H. Guth, D. I. Kaiser, and Y. Nomura, “Inflationary paradigm after Planck 2013,” *Phys. Lett. B* 733 (2014): 112, arXiv:1312.7619 [astro-ph.CO].
 - [7] A. D. Linde, “Inflationary cosmology after Planck 2013,” arXiv:1402.0526 [hep-th].

- [8] J. Martin, “The observational status of cosmic inflation after Planck,” arXiv:1502.05733 [astro-ph.CO].
- [9] G. Steigman, “Primordial nucleosynthesis in the precision cosmology era,” *Ann. Rev. Nucl. Part. Sci.* 57 (2007): 463, arXiv:0712.1100 [astro-ph].
- [10] B. D. Fields, P. Molaro, and S. Sarkar, “Big-bang nucleosynthesis,” *Chin. Phys. C* 38 (2014): 339, arXiv:1412.1408 [astro-ph.CO].
- [11] R. H. Cyburt, B. D. Fields, K. A. Olive, and T.-H. Yeh, “Big bang nucleosynthesis: 2015,” arXiv:1505.01076 [astro-ph.CO].
- [12] P. Adshead, R. Easther, J. Pritchard, and A. Loeb, “Inflation and the scale dependent spectral index: Prospects and strategies,” *JCAP* 1102 (2011): 021, arXiv:1007.3748 [astro-ph.CO].
- [13] L. Dai, M. Kamionkowski, and J. Wang, “Reheating constraints to inflationary models,” *Phys. Rev. Lett.* 113 (2014): 041302, arXiv:1404.6704 [astro-ph.CO].
- [14] P. Creminelli, D. L. Nacir, M. Simonovi, G. Trevisan, and M. Zaldarriaga, “ φ^2 inflation at its endpoint,” *Phys. Rev. D* 90 (2014): 083513, arXiv:1405.6264 [astro-ph.CO].
- [15] J. Martin, C. Ringeval, and V. Vennin, “Observing the inflationary reheating,” *Phys. Rev. Lett.* 114 (2015): 081303, arXiv:1410.7958 [astro-ph.CO].
- [16] J.-O. Gong, G. Leung, and S. Pi, “Probing reheating with primordial spectrum,” *JCAP* 05 (2015): 027, arXiv:1501.03604 [hep-ph].
- [17] R.-G. Cai, Z.-K. Guo, and S.-J. Wang, “Reheating phase diagram for single-field slow-roll inflationary models,” *Phys. Rev. D* 92 (2015): 063506, arXiv:1501.07743 [gr-qc].
- [18] J. L. Cook, E. Dimastrogiovanni, D. A. Easson, and L. M. Krauss, “Reheating predictions in single field inflation,” *JCAP* 04 (2015): 004, arXiv:1502.04673 [astro-ph.CO].
- [19] R. Allahverdi, R. Brandenberger, F.-Y. Cyr-Racine, and A. Mazumdar, “Reheating in inflationary cosmology: Theory and applications,” *Ann. Rev. Nucl. Part. Sci.* 60 (2010): 27, arXiv:1001.2600 [hep-th].
- [20] A. V. Frolov, “Non-linear dynamics and primordial curvature perturbations from preheating,” *Class. Quant. Grav.* 27 (2010): 124006, arXiv:1004.3559 [gr-qc].
- [21] M. A. Amin, M. P. Hertzberg, D. I. Kaiser, and J. Karouby, “Nonperturbative dynamics of reheating after inflation: A review,” *Int. J. Mod. Phys. D* 24 (2015): 1530003, arXiv:1410.3808 [hep-ph].
- [22] M. P. Hertzberg and J. Karouby, “Baryogenesis from the inflaton field,” *Phys. Lett. B* 737 (2014): 34, arXiv:1309.0007 [hep-ph]; M. P. Hertzberg and J. Karouby, “Generating the observed baryon asymmetry from the inflaton field,” *Phys. Rev. D* 89 (2014): 063523, arXiv:1309.0010 [hep-ph].
- [23] P. Adshead and E. I. Sfakianakis, “Leptogenesis from left-handed neutrino production during axion inflation,” arXiv:1508.00881 [hep-ph].
- [24] K. D. Lozanov and M. A. Amin, “End of inflation, oscillons, and matter-antimatter asymmetry,” *Phys. Rev. D* 90 (2014): 083528, arXiv:1408.1811 [hep-ph].
- [25] D. H. Lyth and A. Riotto, “Particle physics models of inflation and the cosmological density perturbation,” *Phys. Rept.* 314 (1999): 1, arXiv:hep-ph/9807278.

- [26] A. Mazumdar and J. Rocher, “Particle physics models of inflation and curvaton scenarios,” *Phys. Rept.* 497 (2011): 85, arXiv:1001.0993 [hep-ph].
- [27] V. Vennin, K. Koyama, and D. Wands, “Encyclopedia Curvatonis,” arXiv:1507.07575 [astro-ph.CO].
- [28] C. G. Callan, Jr., S. R. Coleman, and R. Jackiw, “A new improved energy-momentum tensor,” *Annals. Phys. (N.Y.)* 59 (1970): 42.
- [29] T. S. Bunch, P. Panangaden, and L. Parker, “On renormalization of $\lambda\phi^4$ field theory in curved space-time, I,” *J. Phys. A* 13 (1980): 901; T. S. Bunch and P. Panangaden, “On renormalization of $\lambda\phi^4$ field theory in curved space-time, II,” *J. Phys. A* 13 (1980): 919.
- [30] N. D. Birrell and P. C. W. Davies, *Quantum Fields in Curved Space* (New York: Cambridge University Press, 1982).
- [31] I. L. Buchbinder, S. D. Odintsov, and I. L. Shapiro, *Effective Action in Quantum Gravity* (New York: Taylor and Francis, 1992).
- [32] L. E. Parker and D. J. Toms, *Quantum Field Theory in Curved Spacetime* (New York: Cambridge University Press, 2009).
- [33] D. I. Kaiser, E. A. Mazenc, and E. I. Sfakianakis, “Primordial bispectrum from multifield inflation with nonminimal couplings,” *Phys. Rev. D* 87 (2013): 064004, arXiv:1210.7487 [astro-ph.CO].
- [34] R. N. Greenwood, D. I. Kaiser, and E. I. Sfakianakis, “Multifield dynamics of Higgs inflation,” *Phys. Rev. D* 87 (2013): 044038, arXiv:1210.8190 [hep-ph].
- [35] D. I. Kaiser and E. I. Sfakianakis, “Multifield inflation after Planck: The case for nonminimal couplings,” *Phys. Rev. Lett.* 112 (2014): 011302, arXiv:1304.0363 [astro-ph.CO].
- [36] K. Schutz, E. I. Sfakianakis, and D. I. Kaiser, “Multifield inflation after Planck: Isocurvature modes from nonminimal couplings,” *Phys. Rev. D* 89 (2014): 064044, arXiv:1310.8285 [astro-ph.CO].
- [37] F. L. Bezrukov and M. E. Shaposhnikov, “The Standard Model Higgs boson as the inflaton,” *Phys. Lett. B* 659 (2008): 703, arXiv:0710.3755 [hep-th].
- [38] R. Kallosh and A. Linde, “Non-minimal inflationary attractors,” *JCAP* 1310 (2013): 033, arXiv:1307.7938 [hep-th]; R. Kallosh and A. Linde, “Multi-field conformal cosmological attractors,” *JCAP* 1312 (2013): 006, arXiv:1309.2015 [hep-th]; R. Kallosh, A. Linde, and D. Roest, “Universal attractor for inflation at strong coupling,” *Phys. Rev. Lett.* 112 (2014): 011303, arXiv:1310.3950 [hep-th]; R. Kallosh, A. Linde, and D. Roest, “Superconformal inflationary α -attractors,” *JHEP* 1311 (2013): 198, arXiv:1311.0472 [hep-th]; M. Galante, R. Kallosh, A. Linde, and D. Roest, “The unity of cosmological attractors,” *Phys. Rev. Lett.* 114 (2015): 141302, arXiv:1412.3797 [hep-th]; R. Kallosh and A. Linde, “Planck, LHC, and α -attractors,” *Phys. Rev. D* 91 (2015): 083528, arXiv:1502.07733 [astro-ph.CO]; J. J. M. Carrasco, R. Kallosh, and A. Linde, “Cosmological attractors and initial conditions for inflation,” arXiv:1506.00936 [hep-th].
- [39] B. A. Bassett and S. Liberati, “Geometric reheating after inflation,” *Phys. Rev. D* 58 (1998): 021302, arXiv:hep-ph/9709417.

- [40] S. Tsujikawa, K. Maeda, and T. Torii, “Resonant particle production with non-minimally coupled scalar fields in preheating after inflation,” *Phys. Rev. D* 60 (1999): 063515, arXiv:hep-ph/9901306; S. Tsujikawa, K. Maeda, and T. Torii, “Preheating with non-minimally coupled scalar fields in higher-curvature inflation models,” *Phys. Rev. D* 60 (1999): 123505, arXiv:hep-ph/9906501; S. Tsujikawa, K. Maeda, and T. Torii, “Preheating of the nonminimally coupled inflaton field,” *Phys. Rev. D* 61 (2000): 103501, arXiv:hep-ph/9910214.
- [41] S. Tsujikawa and B. A. Bassett, “A new twist to preheating,” *Phys. Rev. D* 62 (2000): 043510, arXiv:hep-ph/0003068; S. Tsujikawa and B. A. Bassett, “When can preheating affect the CMB?,” *Phys. Lett. B* 536 (2002): 9, arXiv:astro-ph/0204031.
- [42] Y. Watanabe and J. White, “Multi-field formulation of gravitational particle production after inflation,” *Phys. Rev. D* 92 (2015): 023504, arXiv:1503.08430 [astro-ph.CO].
- [43] F. Bezrukov, D. Gorbunov, and M. Shaposhnikov, “On initial conditions for the hot big bang,” *JCAP* 0906 (2009): 029, arXiv:0812.3622 [hep-ph].
- [44] J. García-Bellido, D. G. Figueroa and J. Rubio, “Preheating in the Standard Model with the Higgs-inflaton coupled to gravity,” *Phys. Rev. D* 79 (2009): 063531, arXiv:0812.4624 [hep-ph].
- [45] J.-F. Dufaux, D. G. Figueroa, and J. García-Bellido, “Gravitational waves from Abelian gauge fields and cosmic strings at preheating,” *Phys. Rev. D* 82 (2010): 083518, arXiv:1006.0217 [astro-ph.CO].
- [46] J. García-Bellido, J. Rubio, and M. Shaposhnikov, “Higgs-dilaton cosmology: Are there extra relativistic species?,” *Phys. Lett. B* 718 (2012): 507, arXiv:1209.2119 [hep-ph].
- [47] J. Lachapelle and R. H. Brandenberger, “Preheating with non-standard kinetic term,” *JCAP* 0904 (2009): 020, arXiv:0808.0936 [hep-th].
- [48] J. Karouby, B. Underwood, and A. C. Vincent, “Preheating with the brakes on: The effects of a speed limit,” *Phys. Rev. D* 84 (2011): 043528, arXiv:1105.3982 [hep-th].
- [49] H. L. Child, J. T. Giblin, Jr., R. Ribeiro, and D. Seery, “Preheating with non-minimal kinetic terms,” *Phys. Rev. Lett.* 111 (2013): 051301, arXiv:1305.0561 [astro-ph.CO].
- [50] J. Zhang, Y. Cai, and Y.-S. Piao, “Preheating in a DBI inflation model,” arXiv:1307.6529 [hep-th].
- [51] M. P. DeCross, D. I. Kaiser, A. Prabhu, C. Prescod-Weinstein, and E. I. Sfakianakis, “Preheating after multifield inflation with nonminimal couplings, II: Resonance Structure,” in preparation.
- [52] N. Barnaby, J. Braden, and L. Kofman, “Reheating the universe after multi-field inflation,” *JCAP* 1007 (2010): 016, arXiv:1005.2196 [hep-th].
- [53] D. Battefeld and S. Kawai, “Preheating after N-flation,” *Phys. Rev. D* 77 (2008): 123507, arXiv:0803.0321 [astro-ph]; D. Battefeld, “Preheating after multifield inflation,” *Nucl. Phys. Proc. Suppl.* 192-193 (2009): 126, arXiv:0908.3455 [astro-ph]; D. Battefeld, T. Battefeld, and J. T. Giblin, Jr., “On the suppression of parametric resonance and the viability of tachyonic preheating after multi-field inflation,” *Phys. Rev. D* 79 (2009): 123510, arXiv:0904.2778 [astro-ph.CO]; T. Battefeld, A. Eggemeier, and J. T. Giblin, Jr. “Enhanced preheating after multifield inflation: On the importance of being special,” *JCAP* 11 (2012): 062, arXiv:1209.3301 [astro-ph.CO].

- [54] S. Renaux-Petel and K. Turzynski, “On reaching the adiabatic limit in multi-field inflation,” arXiv:1405.6195 [astro-ph.CO].
- [55] D. I. Kaiser, “Conformal transformations with multiple scalar fields,” Phys. Rev. D 81 (2010): 084044, arXiv:1003.1159 [gr-qc].
- [56] J. M. Bardeen, “Gauge invariant cosmological perturbations,” Phys. Rev. D 22 (1980): 1882.
- [57] V. F. Mukhanov, “Quantum theory of gauge invariant cosmological perturbations,” Sov. Phys. JETP 67 (1988): 1297.
- [58] H. Kodama and M. Sasaki, “Cosmological perturbation theory,” Prog. Theor. Phys. Suppl. 78 (1984): 1.
- [59] V. F. Mukhanov, H. A. Feldman, and R. H. Brandenberger, “Theory of cosmological perturbations,” Phys. Rept. 215 (1992): 203.
- [60] K. A. Malik and D. Wands, “Cosmological perturbations,” Phys. Rept. 475 (2009): 1, arXiv:0809.4944 [astro-ph].
- [61] M. Sasaki and E. D. Stewart, “A general analytic formula for the spectral index of the density perturbations produced during inflation,” Prog. Theo. Phys. 95 (1996): 71, arXiv:astro-ph/9507001.
- [62] C. Gordon, D. Wands, B. A. Bassett, and R. Maartens, “Adiabatic and entropy perturbations from inflation,” Phys. Rev. D 63 (2001): 023506, arXiv:astro-ph/0009131.
- [63] S. Groot Nibbelink and B. J. W. van Tent, “Density perturbations arising from multiple field slow-roll inflation,” arXiv:hep-ph/0011325; “Scalar perturbations during multiple-field slow-roll inflation,” Class. Quant. Grav. 19 (2002): 613, arXiv:hep-ph/0107272.
- [64] D. Wands, N. Bartolo, S. Matarrese, and A. Riotto, “An observational test of two-field inflation,” Phys. Rv. D 66 (2002): 043520, arXiv:astro-ph/0205253.
- [65] D. Seery and J. E. Lidsey, “Primordial non-Gaussianities from multiple-field inflation,” JCAP 0509 (2005): 011, arXiv:astro-ph/0506056.
- [66] H.-C. Lee, M. Sasaki, E. D. Stewart, T. Tanaka, and S. Yokoyama, “A new delta N formalism for multi-component inflation,” JCAP 0510 (2005): 004, arXiv:astro-ph/0506262.
- [67] D. Wands, “Multiple field inflation,” Lect. Notes Phys. 738 (2008): 275, arXiv:astro-ph/0702187.
- [68] S. Yokoyama, T. Suyama, and T. Tanaka, “Primordial non-Gaussianity in multi-scalar slow-roll inflation,” JCAP 0707 (2007): 013, arXiv:0705.3178 [astro-ph]; “Primordial non-Gaussianity in multi-scalar inflation,” Phys. Rev. D 77 (2008): 083511, arXiv:0711.2920 [astro-ph].
- [69] D. Langlois and S. Renaux-Petel, “Perturbations in generalized multi-field inflation,” JCAP 0804 (2008): 017, arXiv:0801.1085 [hep-th].
- [70] C. M. Peterson and M. Tegmark, “Testing two-field inflation,” Phys. Rev. D 83 (2011): 023522, arXiv:1005.4056 [astro-ph.CO]; “Non-Gaussianity in two-field inflation,” Phys. Rev. D 84 (2011): 023520, arXiv:1011.6675 [astro-ph.CO]; “Testing multi-field inflation: A geometric approach,” arXiv:1111.0927 [astro-ph.CO].

- [71] J.-O. Gong and T. Tanaka, “A covariant approach to general field space metric in multifield inflation,” JCAP 1103 (2011): 015, arXiv:1101.4809 [astro-ph.CO].
- [72] J. Elliston, D. Seery, and R. Tavakol, “The inflationary bispectrum with curved field-space,” JCAP 1211 (2012): 060, arXiv:1208.6011 [astro-ph.CO].
- [73] A. O. Barvinsky, A. Yu. Kamenshchik, C. Kiefer, A. A. Starobinsky, and C. F. Steinwachs, “Asymptotic freedom in inflationary cosmology with a nonminimally coupled Higgs field,” JCAP 0912 (2009): 003, arXiv:0904.1698 [hep-ph]; “Higgs boson, renormalization group, and naturalness in cosmology,” Euro. Phys. J. C 72 (2012): 2219, arXiv:0910.1041 [hep-ph].
- [74] F. Bezrukov, M. Yu. Kalmykov, B. A. Kniehl, and M. E. Shaposhnikov, “Higgs boson mass and new physics,” JHEP 1210 (2012): 140, arXiv:1205.2893 [hep-ph].
- [75] K. Allison, “Higgs ξ -inflation for the 125 -126 GeV Higgs: A two-loop analysis,” arXiv:1306.6931 [hep-ph].
- [76] I. G. Moss, “Vacuum stability and the scaling behaviour of the Higgs-curvature coupling,” arXiv:1509.03554 [hep-th].
- [77] T. Futamase and K. Maeda, “Chaotic inflationary scenario of the Universe with a nonminimally coupled ‘inflaton’ field,” Phys. Rev. D 39 (1989): 399.
- [78] D. S. Salopek, J. R. Bond, and J. M. Bardeen, “Designing density fluctuation spectra in inflation,” Phys. Rev. D 40 (1989): 1753.
- [79] R. Fakir, S. Habib, and W. G. Unruh, “Cosmological density perturbations with modified gravity,” Astrophys. J. 394 (1992): 396; R. Fakir and W. G. Unruh, “Improvement on cosmological chaotic inflation through nonminimal coupling,” Phys. Rev. D 41 (1990): 1783.
- [80] N. Makino and M. Sasaki, “The density perturbation in the chaotic inflation with nonminimal coupling,” Prog. Theor. Phys. 86 (1991): 103.
- [81] D. I. Kaiser, “Primordial spectral indices from generalized Einstein theories,” Phys. Rev. D 52 (1995): 4295, arXiv:astro-ph/9408044.
- [82] P. A. R. Ade et al. (BICEP2/Keck and Planck collaborations), “A joint analysis of BICEP2/Keck array and Planck data,” Phys. Rev. Lett. 114 (2015): 101301, arXiv:1502.00612 [astro-ph]; P. A. R. Ade et al. (Planck collaboration), “Planck 2015 results, XIII: Cosmological parameters,” arXiv:1502.01589 [astro-ph].
- [83] F. C. Adams, K. Freese, and A. H. Guth, “Constraints on the scalar-field potential in inflationary models,” Phys. Rev. D 43 (1991): 965.
- [84] D. I. Kaiser, “Constraints in the context of induced gravity inflation,” Phys. Rev. D 49 (1994): 6347, arXiv:astro-ph/9308043.
- [85] A. H. Guth and E. I. Sfakianakis, “Density Perturbations in Hybrid Inflation Using a Free Field Theory Time-Delay Approach,” arXiv:1210.8128 [astro-ph.CO].
- [86] X. Chen, M. H. Namjoo and Y. Wang, “Quantum Primordial Standard Clocks,” arXiv:1509.03930 [astro-ph.CO].

- [87] X. Chen, M. H. Namjoo and Y. Wang, “Models of the Primordial Standard Clock,” JCAP **1502**, no. 02, 027 (2015) [arXiv:1411.2349 [astro-ph.CO]].
- [88] X. Chen and M. H. Namjoo, “Standard Clock in Primordial Density Perturbations and Cosmic Microwave Background,” Phys. Lett. B **739**, 285 (2014) [arXiv:1404.1536 [astro-ph.CO]].
- [89] X. Chen and C. Ringeval, “Searching for Standard Clocks in the Primordial Universe,” JCAP **1208**, 014 (2012) [arXiv:1205.6085 [astro-ph.CO]].
- [90] M. S. Turner, “Coherent scalar field oscillations in an expanding universe,” Phys. Rev. D **28** (1983): 1243.
- [91] E.ourgoulhon and S. Bonazzola, “A formulation of the virial theorem in general relativity,” Class. Quant. Grav. **11** (1994): 443.
- [92] D. I. Kaiser, “Post-inflation reheating in an expanding universe,” Phys. Rev. D **53** (1996): 1776, arXiv:astro-ph/9507108.
- [93] D. Boyanovsky, H. J. de Vega, R. Holman, and J. Salgado, “Analytic and numerical study of preheating dynamics,” Phys. Rev. D **54** (1996): 7570, arXiv:hep-ph/9608205.
- [94] D. I. Kaiser, “Preheating in an expanding universe: Analytic results for the massless case,” Phys. Rev. D **56** (1997): 706, arXiv:hep-ph/9702244; D. I. Kaiser, “Resonance structure for preheating with massless fields,” Phys. Rev. D **57** (1998): 702, arXiv:hep-ph/9707516.
- [95] P. Greene, L. Kofman, A. Linde, and A. Starobinsky, “Structure of resonance in preheating after inflation,” Phys. Rev. D **56** (1997): 6175, arXiv:hep-ph/9705347.
- [96] M. Abramowitz and I. Stegun, eds., *Handbook of Mathematical Functions* (New York: Dover, 1965).
- [97] S. Weinberg, *Cosmology* (New York: Oxford University Press, 2008).
- [98] S. Carroll, *Spacetime and Geometry* (New York: Addison-Wesley, 2004).
- [99] L. Kofman, A. Linde, and A. Starobinsky, “Towards the theory of reheating after inflation,” Phys. Rev. D **56** (1997): 3258, arXiv:hep-ph/9704452.
- [100] B. A. Bassett, F. Tamburini, D. I. Kaiser, and R. Maartens, “Metric preheating and limitations of linearized gravity,” Nucl. Phys. B **561** (1999): 188, arXiv:hep-ph/9901319.
- [101] M. P. Hertzberg, J. Karouby, W. G. Spitzer, J. C. Becerra, and L. Li, “A theory of self-resonance after inflation, Part 1: Adiabatic and isocurvature Goldstone modes,” Phys. Rev. D **90** (2014): 123528, arXiv:1408.1396 [hep-th]; M. P. Hertzberg, J. Karouby, W. G. Spitzer, J. C. Becerra, and L. Li, “A theory of self-resonance after inflation, Part 2: Quantum mechanics and particle-antiparticle asymmetry,” Phys. Rev. D **90** (2014): 123529, arXiv:1408.1398 [hep-th].
- [102] B. R. Greene, T. Prokopec, and T. G. Roos, “Inflation decay and heavy particle production with negative coupling,” Phys. Rev. D **56** (1997): 6484, arXiv:hep-ph/9705357.
- [103] B. A. Bassett, C. Gordon, R. Maartens, and D. I. Kaiser, “Restoring the sting to metric preheating,” Phys. Rev. D **61** (2000): 061302, arXiv:hep-ph/9909482.
- [104] M. Gleiser, “Pseudo-stable bubbles,” Phys. Rev. D **49** (1994): 2978, arXiv:hep-ph/9308279; E. J. Copeland, M. Gleiser, and H.-R. Mueller, “Oscillons: Resonant configurations during bubble collapse,”

Phys. Rev. D 52 (1995): 1920, arXiv:hep-ph/9503217.

- [105] M. A. Amin, R. Easther, and H. Finkel, “Inflaton fragmentation and oscillon formation in three dimensions,” JCAP 1012 (2010): 001, arXiv:1009.2505 [astro-ph.CO]; M. A. Amin, R. Easther, H. Finkel, R. Flauger, and H. P. Hertzberg, “Oscillons after inflation,” Phys. Rev. Lett. 108 (2012): 241302, arXiv:1106.3335 [astro-ph.CO].